

A powerful matrix formalism for stress singularities in anisotropic multi-material corners. Homogeneous (orthogonal) boundary and interface conditions

María A. Herrera-Garrido, Vladislav Mantič*, Alberto Barroso

Grupo de Elasticidad y Resistencia de Materiales, Escuela Técnica Superior de Ingeniería, Universidad de Sevilla, Camino de los Descubrimientos s/n, 41092 Sevilla, Spain

ARTICLE INFO

Keywords:

Corner singularity
Singularity exponent
Anisotropic linear elastic material
Homogeneous boundary and interface conditions
Frictionless contact
Stroh formalism

ABSTRACT

A computational code based on a semianalytic procedure for the determination of the characteristic exponents and the singular stress and displacement fields in multi-material corners is developed. Linear elastic anisotropic materials under generalized plane strain state are considered. This code is a universal computational tool able to analyze both open and closed (periodic) corners, composed of one or multiple materials with isotropic, transversely isotropic or orthotropic constitutive laws, covering both mathematically non-degenerate and degenerate materials in the framework of Stroh formalism. In multi-material corners, material junctions with perfectly bonded or frictionless sliding interfaces can be studied. The considered homogeneous boundary conditions cover stress free and fixed faces, or faces with some restricted or allowed direction of displacements, defined either in the reference frame aligned with the cylindrical coordinate system or in an inclined reference frame. The code is developed in MATLAB and it is based on the Stroh matrix formalism for anisotropic elasticity, the concept of transfer matrix for single material wedges, and on the matrix formalism for homogeneous (orthogonal) boundary conditions. The comparison of the characteristic exponents obtained by the present code and by the solution of closed-form eigenequations available in the literature, has a two-fold objective, first to exhaustively check the general computational implementation of the matrix formalism presented, and second to check the closed-form expressions of eigenequations for relevant specific cases published in the literature.

1. Introduction

Stress singularities, also referred to as singular stresses, i.e. unbounded stresses, take place in linear elastic structures due to some discontinuities, such as non-smooth geometry (e.g., cracks or V-notches), jumps in kind or in values of boundary or interface conditions, and jumps in material properties (e.g., joints of dissimilar materials, interface cracks). Points (or edges in 3D view) where such discontinuities originate singular stresses are called singular points (or singular edges, e.g. crack fronts). These points are prone to failure initiation due to high stress values in their neighborhood, which is generally referred to as a corner. The singular point itself is called a corner tip. A configuration where several materials meet at a singular point is called a multi-material corner.

The most relevant early studies of stress singularities in isotropic and single-material corners, with free or fixed boundaries, by Wieghardt [1] and Williams [2], see Vasilopoulos [3] for a careful review, were generalized in a large number of later works. In particular,

many analytical, semi-analytical and numerical approaches have been proposed for the study of stress singularities in multi-material corners. Numerical approaches, such as those developed in [4,5], are more general, as they can solve some stress singularity problems that cannot be solved by analytical or semi-analytical approaches. However, analytical or semi-analytical approaches, such as those developed in [6] for isotropic materials and in [7,8] for anisotropic materials, which provide an explicit closed-form expression of the characteristic corner equation (eigenequation), usually lead to higher accuracy of results. Thus, in the present study, a novel semi-analytical approach is developed and implemented in a computational code. For the sake of brevity, we will often refer to single-material wedge as a *material* and to multi-material wedge with perfectly bonded materials simply as a *wedge*.

For isotropic bi-material and tri-material corners, basic eigenequations were deduced, e.g., in [9–11]. A semi-analytic procedure for isotropic multi-material corners was introduced by Dempsey and Sinclair [6]. One of the earliest studies of corner singularities in anisotropic

* Corresponding author.

E-mail address: mantic@us.es (V. Mantič).

materials were those by Bogy [12,13], analyzing singular stresses in anisotropic single and bi-material corners, and by Ting and Chou [14], paying attention to configurations with multiple (repeated) roots of the characteristic equation of an anisotropic material (so-called mathematically degenerate materials) and also with multiple roots of the corner eigenequation.

In the last 20 years, many authors have focused their studies on anisotropic multi-material corners. Costabel et al. [7] developed a semi-analytic code for the computation of stress singularities for elastic multi-material corner problems with perfectly bonded interfaces and with single roots of the material characteristic equation (so-called mathematically non-degenerate materials). Wu [15] used the Stroh formalism to deduce eigenequations for non-homogeneous anisotropic corners with a wide range of boundary conditions, but not including frictional contact. In 2003, several related approaches for singularity analysis of anisotropic multi-material corners with perfectly bonded interfaces were developed, using the Stroh formalism [16,17], by Hwu et al. [18] for mathematically non-degenerate materials, and by Yin [19] and Barroso et al. [20] for both mathematically non-degenerate and degenerate materials. In particular, the code implemented in [20] by using the computer algebra software Mathematica [21] was able to calculate characteristic exponents for any multi-material open or closed (periodic) corner in generalized plane strain, considering perfectly bonded interfaces, with free or clamped boundary faces. The great novelty of this code was that for the first time it was possible to analyze corners with mathematically non-degenerate, degenerate (e.g., isotropic) and extraordinarily degenerate materials. The procedure presented in [20] was further developed by Mantič et al. [8], who introduced a general matrix formalism able to analyze multi-material corners problems with many different boundary conditions, including also frictional contact for boundary and interface conditions, and with any kind of linear elastic materials.

The present paper applies and further develops the general matrix formalism for singularity analysis of multi-material corners introduced in [8]. The description of this formalism in [8] was very concise, which in view of its generality and complexity could make difficult its comprehension by readers. Furthermore this matrix formalism has not been verified so far by its full computational implementation, except by ad hoc implementations for some specific cases studied in [8].

Therefore, the aim of the present paper is to present this matrix formalism in a comprehensive way for the case of homogeneous and orthogonal boundary and interface conditions (i.e. omitting friction contact, which makes its presentation much simpler), revise this matrix formalism and provide complementary and clarifying explanations. However, the most relevant contribution of this paper is the first fully general implementation of the formalism introduced in [8], and a comprehensive checking of this implementation by comparing its results with the numerous analytical and numerical results of corner singularity analysis available in the literature. In a forthcoming paper, boundary and interface conditions with frictional sliding contact will be included in the present matrix formalism, and its computational implementation will be described together with some examples of its successful testing.

Although some corner problems lead to eigenequations with multiple (repeated) roots, and such configurations were studied by Dempsey and Sinclair [6] for isotropic materials, and by Ting and Chou [14], Wu [15] and Steigemann [22] for anisotropic materials, the present paper is limited to single roots of the corner eigenequation, for the sake of simplicity.

The present paper presents a new code developed in Matlab [23], which is based on the previous one [20]. The possibility to consider interfaces between the materials in the corner with frictionless sliding, and several boundary conditions with allowed or restricted displacement directions have been added to this code, see Fig. 1 for the notation used to describe a multi-material corner. The possibility of sliding between materials implies that the size of the matrix to be solved is not

always 3×3 or 6×6 , but $6W \times 6W$, where W is the number of wedges formed by angular sectors of materials perfectly bonded together.

The following ingredients are key in the development of the present matrix formalism:

- Stroh formalism for anisotropic elasticity [16,17]
- Transfer matrix for a single-material wedge proposed by Ting [24]
- Matrix formalism for homogeneous orthogonal boundary and interface conditions proposed by Mantič et al. [8].

We speak about homogeneous orthogonal boundary conditions when the stress and displacement vectors are orthogonal to each other. This happens when there is a coordinate system in which always one of the components of one of these vectors is null. This means, when the displacement in one direction is restricted (equal to zero), the stress is allowed, and when the displacement is allowed in one direction, the stress will vanish in that direction. For example, in the symmetry boundary condition the displacement in the normal direction is zero $u_n = 0$, but the normal stress component is in general non zero $\sigma_n \neq 0$.

The content of this paper is divided into sections according to the steps that the implemented computer code follows: Material characterization by applying first the Stroh formalism in Section 2, and then computing the transfer matrix in Section 3. In the next step we obtain the boundary and interface matrices employing the matrix formalism for homogeneous orthogonal boundary and interface conditions presented in Section 4. In Section 5, all these matrices are assembled to form the characteristic matrix of the corner defining a nonlinear eigensystem. The numerical solution of this eigensystem gives the characteristic exponents. For some special cases such as single-material and bi-material corners, reduced eigensystems are deduced. The characteristic angular functions of stresses and displacements are calculated individually for each characteristic exponent in Section 6. The entire implementation is summarized in Section 7. Finally, in Section 8, many numerical examples are shown in order to check our own code and also the closed-form eigenequations presented by other authors. These examples include several relevant cases such as V-notches, interface cracks, cracks meeting interface, multi-material closed corners.

Noteworthy, the present code can be used to test new analytic formulas for the characteristic exponents or eigenequations developed for relevant engineering problems, which are very suitable for practical applications and parametric studies.

2. Stroh formalism applied to stress singularity analysis of linear elastic anisotropic materials

Stroh formalism is a powerful tool to solve linear anisotropic elastic problems. This formalism is based on the equilibrium equations in terms of displacements (in the absence of body forces) obtained by using the constitutive law of linear anisotropic elasticity,

$$\sigma_{ij} = C_{ijkl} \epsilon_{kl} = C_{ijkl} u_{k,l}, \quad (1)$$

$$C_{ijkl} u_{k,lj} = 0, \quad (2)$$

where C_{ijkl} is the positive definite ($C_{ijkl} \epsilon_{ij} \epsilon_{kl} > 0$ for non zero $\epsilon_{ij} = \epsilon_{ji}$) and symmetric fourth-order tensor of elastic stiffnesses ($C_{ijkl} = C_{jikl} = C_{klij}$), σ_{ij} is the Cauchy stress tensor, u_i the displacement field and ϵ_{ij} the small strain tensor. Assuming a generalized plane strain state, where the displacements u_i depend exclusively on the coordinates x_1 and x_2 , $u_i(x_1, x_2)$, we consider a solution of the system of Eqs. (2) in the following form

$$u_k(x_1, x_2) = a_k f(z), \quad (3)$$

$$z = x_1 + px_2, \quad (4)$$

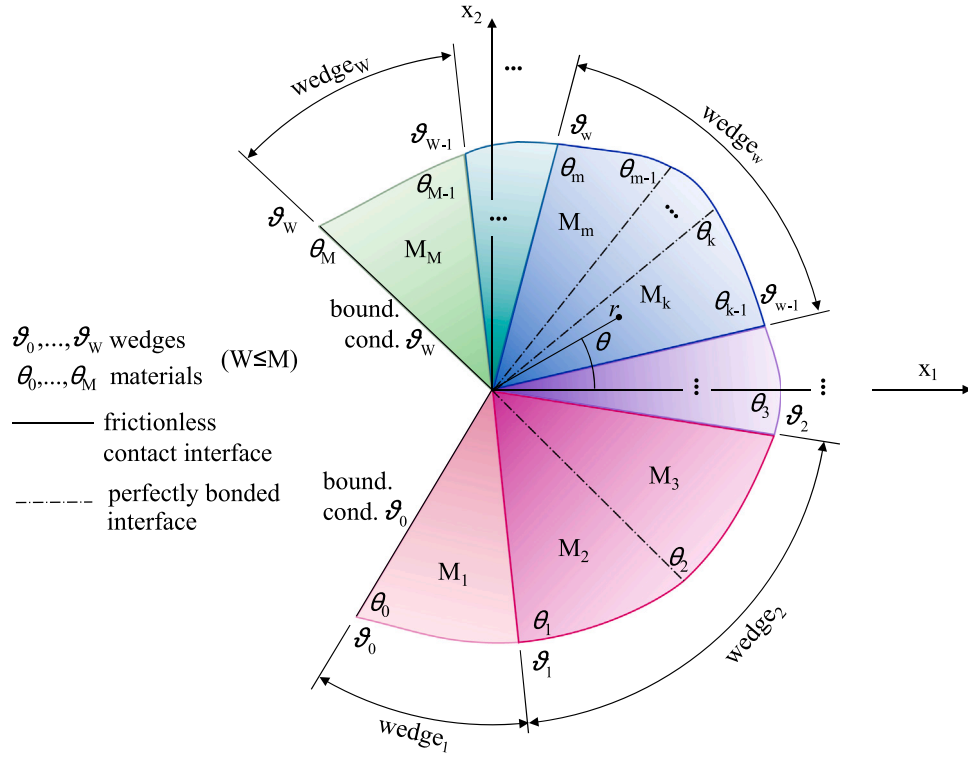


Fig. 1. Multi-material corner notation (2D view).

where $f(z)$ is an analytic function of a variable z given by a linear combination of x_1 and x_2 , and p and a_i are constants to be determined. Taking into account the geometry of the present corner problem (Fig. 1), it will be useful to employ z written in polar coordinates

$$z = r(\cos(\theta) + p \sin(\theta)). \tag{5}$$

Differentiating twice the expression (3) with respect to x_i and x_j and substituting in (2), we obtain the quadratic eigenvalue problem for the number p and the vector \mathbf{a}

$$[C_{i1k1} + p(C_{i1k2} + C_{i2k1}) + p^2 C_{i2k2}]a_k = 0. \tag{6}$$

To write this eigenvalue problem in matrix form, we define the following matrices (second-order tensors)

$$Q_{ik} = C_{i1k1}, \quad R_{ik} = C_{i1k2}, \quad T_{ik} = C_{i2k2}. \tag{7}$$

Then, the quadratic eigenvalue problem (6) is written as

$$[\mathbf{Q} + p(\mathbf{R} + \mathbf{R}^T) + p^2 \mathbf{T}]\mathbf{a} = \mathbf{0}. \tag{8}$$

A non trivial solution for \mathbf{a} may exist only if the determinant of the matrix in this linear system is zero,

$$\det(\mathbf{Q} + p(\mathbf{R} + \mathbf{R}^T) + p^2 \mathbf{T}) = 0. \tag{9}$$

This equation is known as the Lekhnitskii–Stroh sextic polynomial equation in p for anisotropic materials under generalized plane strain [25]. Lekhnitskii [26] showed that the six dimensionless roots of this equation p_α ($\alpha = 1, \dots, 6$), called also *eigenvalues*, are complex, i.e. $p_\alpha \in \mathbb{C}$. In the present paper, we will assume the following ordering of these six eigenvalues according to the sign of their imaginary part

$$\text{Im } p_\alpha > 0, \quad p_{\alpha+3} = \bar{p}_\alpha, \quad \alpha = 1, 2, 3, \tag{10}$$

where Im denotes the imaginary part and the overbar denotes the complex conjugate value. For an eigenvalue p_α , the associated eigenvector \mathbf{a}_α can be obtained from the linear system (8).

The stress tensor components σ_{i1} and σ_{i2} can be obtained by the following expressions

$$\sigma_{i1} = (Q_{ik} + pR_{ik})a_k f'(z), \tag{11}$$

$$\sigma_{i2} = (R_{ki} + pT_{ik})a_k f'(z), \tag{12}$$

while σ_{33} is obtained from the constitutive law by taking into account that $\epsilon_{33} = 0$. Expressions (11) and (12) can be rewritten as

$$\sigma_{i1} = -pb_i f'(z), \quad \sigma_{i2} = b_i f'(z), \tag{13}$$

where the eigenvector \mathbf{b} is obtained from the eigenvector \mathbf{a} as

$$\mathbf{b} = (\mathbf{R}^T + p\mathbf{T})\mathbf{a} = -\frac{1}{p}(\mathbf{Q} + p\mathbf{R})\mathbf{a}. \tag{14}$$

The eigenvectors \mathbf{a}_α and \mathbf{b}_α are ordered according to the ordering of p_α in (10)

$$\mathbf{a}_{\alpha+3} = \bar{\mathbf{a}}_\alpha \quad \text{and} \quad \mathbf{b}_{\alpha+3} = \bar{\mathbf{b}}_\alpha, \quad \alpha = 1, 2, 3. \tag{15}$$

By introducing the stress function vector $\boldsymbol{\varphi}$ as

$$\varphi_i = b_i f(z), \quad \text{or in matrix notation} \quad \boldsymbol{\varphi} = \mathbf{b}f(z), \tag{16}$$

the expressions (13) take the following form

$$\sigma_{i1} = -\varphi_{i,2}, \quad \sigma_{i2} = \varphi_{i,1}. \tag{17}$$

The stress function vector $\boldsymbol{\varphi}$ represents, together with the displacement vector \mathbf{u} , the main variables of the Stroh formalism.

For mathematically non-degenerate materials, i.e. those with the six different eigenvalues p_α , we can superimpose the six solutions for displacement vector from (3), and the corresponding six solutions for the stress function vector from (16), giving, in view of (15),

$$\mathbf{u}(x_1, x_2) = \sum_{\alpha=1}^3 \mathbf{a}_\alpha f_\alpha(z_\alpha) + \bar{\mathbf{a}}_\alpha f_{\alpha+3}(\bar{z}_\alpha), \tag{18}$$

$$\boldsymbol{\varphi}(x_1, x_2) = \sum_{\alpha=1}^3 \mathbf{b}_\alpha f_\alpha(z_\alpha) + \bar{\mathbf{b}}_\alpha f_{\alpha+3}(\bar{z}_\alpha). \tag{19}$$

Analogous fundamental representations of the Stroh formalism of the displacement and stress function vectors for degenerate materials, with multiple eigenvalues p_α , can be found in [8,19,20,27].

For corner singularity analysis, the following expressions will be considered in the neighborhood of the corner vertex

$$f_\alpha(z_\alpha) = z_\alpha^\lambda q_\alpha, \quad f_{\alpha+3}(\bar{z}_\alpha) = \bar{z}_\alpha^\lambda \bar{q}_\alpha, \quad (20)$$

with no summation over α , and where λ is the dimensionless characteristic exponent, related with the stress singularity order δ by $\delta = 1 - \lambda$. To keep the strain energy bounded, and the resultant forces along the radial lines to be finite in the neighborhood of the corner tip, the real part of λ must be non-negative, $\text{Re}(\lambda) \geq 0$. Rigid body translations correspond to $\lambda = 0$.

Although, according to the mathematical theory of linear elliptic systems [22,28,29], the general expression of f_α may involve also positive integer powers of a logarithmic term

$$f_\alpha(z_\alpha) = z_\alpha^\lambda \log^p z_\alpha q_\alpha, \quad \text{with } p = 0, 1, 2, \dots \quad (21)$$

in the present paper only power-law singularities (20) will be considered for the sake of simplicity.

Substituting (20) in the representations (18) and (19) gives

$$\mathbf{u} = \mathbf{A} \langle z_*^\lambda \rangle \mathbf{q} + \bar{\mathbf{A}} \langle \bar{z}_*^\lambda \rangle \bar{\mathbf{q}}, \quad (22)$$

$$\boldsymbol{\varphi} = \mathbf{B} \langle z_*^\lambda \rangle \mathbf{q} + \bar{\mathbf{B}} \langle \bar{z}_*^\lambda \rangle \bar{\mathbf{q}}, \quad (23)$$

where the column vectors of matrices \mathbf{A} and \mathbf{B} are the eigenvectors \mathbf{a}_α and \mathbf{b}_α , respectively,

$$\mathbf{A} = [\mathbf{a}_1, \mathbf{a}_2, \mathbf{a}_3], \quad \mathbf{B} = [\mathbf{b}_1, \mathbf{b}_2, \mathbf{b}_3], \quad (24)$$

and $\langle z_*^\lambda \rangle$ denotes a diagonal matrix

$$\langle z_*^\lambda \rangle = \text{diag}(z_1^\lambda, z_2^\lambda, z_3^\lambda). \quad (25)$$

By using (5) we get

$$z_\alpha = r(\cos(\theta) + p_\alpha \sin(\theta)) = r \zeta_\alpha(\theta), \quad (26)$$

and substituting in (25)

$$\langle z_*^\lambda \rangle = r^\lambda \text{diag}(\zeta_1^\lambda(\theta), \zeta_2^\lambda(\theta), \zeta_3^\lambda(\theta)). \quad (27)$$

By substituting this expression in (22) and (23) we obtain

$$\mathbf{u} = r^\lambda \{ \mathbf{A} \langle \zeta_*^\lambda \rangle \mathbf{q} + \bar{\mathbf{A}} \langle \bar{\zeta}_*^\lambda \rangle \bar{\mathbf{q}} \}, \quad (28)$$

$$\boldsymbol{\varphi} = r^\lambda \{ \mathbf{B} \langle \zeta_*^\lambda \rangle \mathbf{q} + \bar{\mathbf{B}} \langle \bar{\zeta}_*^\lambda \rangle \bar{\mathbf{q}} \}. \quad (29)$$

These representations can be written in a compact way as

$$\mathbf{w}(r, \theta) = r^\lambda \mathbf{XZ}^\lambda \mathbf{t}, \quad (30)$$

where:

$$\mathbf{w}(r, \theta) = \begin{bmatrix} \mathbf{u}(r, \theta) \\ \boldsymbol{\varphi}(r, \theta) \end{bmatrix}, \quad \mathbf{X} = \begin{bmatrix} \mathbf{A} & \bar{\mathbf{A}} \\ \mathbf{B} & \bar{\mathbf{B}} \end{bmatrix}, \quad \mathbf{Z}^\lambda(\theta) = \begin{bmatrix} \langle \zeta_\alpha^\lambda(\theta) \rangle & \mathbf{0} \\ \mathbf{0} & \langle \bar{\zeta}_\alpha^\lambda(\theta) \rangle \end{bmatrix}, \quad (31)$$

$$\mathbf{t} = \begin{bmatrix} \mathbf{q} \\ \bar{\mathbf{q}} \end{bmatrix}.$$

For expressions analogous to (30) and (31) for mathematically degenerate materials, see [8,19,20].

3. Singular elastic solution in a single-material wedge. Transfer matrix

Considering the special geometry of singularity problems for multi-material corners, the *transfer matrix* concept proposed by Ting [24] is very helpful to simplify the problem analysis.

In the case of a single-material wedge of number m , this matrix allows us to get a relation between displacements and the stress function vector, \mathbf{u} and $\boldsymbol{\varphi}$, on both faces of the wedge. That is, the transfer matrix \mathbf{E}_m , that depends on the material properties, single-material wedge

angles (θ_m, θ_{m-1}) and singularity exponent λ , relates $\mathbf{w}_m(r, \theta_{m-1})$ with $\mathbf{w}_m(r, \theta_m)$ in the following way:

$$\mathbf{w}_m(r, \theta_m) = \mathbf{E}_m(\lambda, \theta_m, \theta_{m-1}) \mathbf{w}_m(r, \theta_{m-1}). \quad (32)$$

The matrix \mathbf{E}_m , for mathematically non-degenerate materials, is given by

$$\mathbf{E}_m(\lambda, \theta_m, \theta_{m-1}) = \mathbf{XZ}^\lambda(\theta_m, \theta_{m-1})\mathbf{X}^{-1}, \quad (33)$$

where

$$\mathbf{Z}^\lambda(\theta_m, \theta_{m-1}) = \begin{bmatrix} \langle \zeta_\alpha^\lambda(\theta_m, \theta_{m-1}) \rangle & 0 \\ 0 & \langle \bar{\zeta}_\alpha^\lambda(\theta_m, \theta_{m-1}) \rangle \end{bmatrix}, \quad (34)$$

and

$$\zeta_\alpha(\theta_m, \theta_{m-1}) = \cos(\theta_m - \theta_{m-1}) + p_\alpha(\theta_{m-1}) \sin(\theta_m - \theta_{m-1}), \quad (35)$$

with

$$p_\alpha(\theta_{m-1}) = \frac{p_\alpha \cos(\theta_{m-1}) - \sin(\theta_{m-1})}{p_\alpha \sin(\theta_{m-1}) + \cos(\theta_{m-1})}. \quad (36)$$

Analogous expressions for degenerate and extraordinary degenerate materials can be found in [8,20]

Continuity problems can arise when evaluating the complex power function $\zeta_\alpha^\lambda(\theta_m, \theta_{m-1})$ for which a proper choice of branch cut is necessary. Taking into account that $0 < \theta_m - \theta_{m-1} \leq 2\pi$, and $\text{Im}(p_\alpha(\theta)) > 0$ for $\alpha = 1, 2, 3$, we use in our code the following argument function ψ and radius ρ

$$\psi = \arg(\zeta_\alpha(\theta_m, \theta_{m-1})) \in (0, 2\pi), \quad \rho = |\zeta_\alpha(\theta_m - \theta_{m-1})| \quad (37)$$

in the (real variable) expansion of the complex power function

$$\zeta_\alpha^\lambda(\theta_m, \theta_{m-1}) = \rho^{\text{Re}(\lambda)} e^{-\psi \text{Im}(\lambda)} [\cos(\text{Re}(\lambda)\psi + \text{Im}(\lambda) \ln \rho) + i \sin(\text{Re}(\lambda)\psi + \text{Im}(\lambda) \ln \rho)] \quad (38)$$

valid for any programming language. An equivalent possibility to avoid the continuity problem when coding in Matlab is presented in [30, Section 4.4.1].

For the sake of notation simplicity, hereafter $\mathbf{E}_m(\lambda, \theta_m, \theta_{m-1})$ will be denoted as $\mathbf{E}_m(\lambda)$.

4. Matrix formalism for boundary and interface conditions

4.1. Reference frame attached to a wedge face

To define the boundary and interface conditions, it is first necessary to choose a suitable reference frame for the displacement and traction vectors, which facilitates the further development of the present matrix formalism. For this purpose, an orthonormal basis of vectors attached to the corner faces has been chosen as defined in [8], see Fig. 2

$$(\mathbf{s}_r(\vartheta), \mathbf{s}_3, \mathbf{n}(\vartheta)), \quad (39)$$

with Cartesian components

$$\mathbf{s}_r(\vartheta) = \begin{pmatrix} -\cos \vartheta \\ -\sin \vartheta \\ 0 \end{pmatrix}, \quad \mathbf{s}_3 = \begin{pmatrix} 0 \\ 0 \\ 1 \end{pmatrix}, \quad \mathbf{n}(\vartheta) = \begin{pmatrix} -\sin \vartheta \\ \cos \vartheta \\ 0 \end{pmatrix}. \quad (40)$$

These unique right-handed reference frames at each boundary face or interface $(\mathbf{s}_r(\vartheta), \mathbf{s}_3(\vartheta), \mathbf{n}(\vartheta))$ are defined for the imposition of boundary or interface conditions, for both displacement and stress function vectors. The vector \mathbf{s}_r should be used with caution in (41), where the vector \mathbf{s} is considered always as counterclockwise on a solid boundary, whereas the direction of \mathbf{s}_r on a wedge face can be clockwise or counterclockwise.

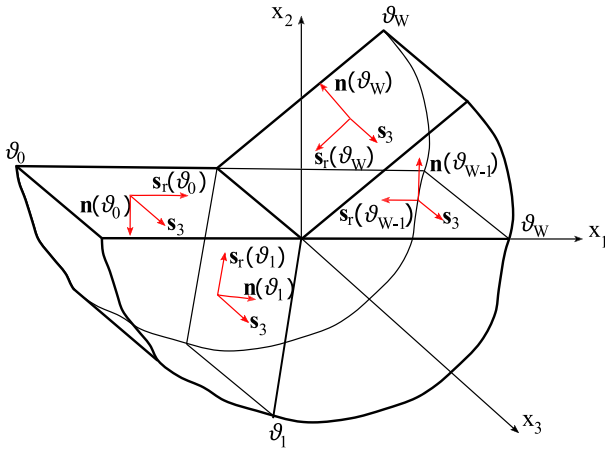


Fig. 2. Orthonormal basis attached to each face.

4.2. Boundary condition matrices

As follows from the introduction section, the homogeneous boundary conditions considered in the present paper fulfill the orthogonality condition between the boundary traction and displacement vectors. Therefore, there is a Cartesian coordinate system in which if a component of the stress function vector φ is not zero then that component of the displacement vector \mathbf{u} is zero, and vice versa.

Considering that the traction vector \mathbf{t} at a point (x_1, x_2) can be calculated as the tangential derivative of the stress function vector φ with respect to the tangential vector \mathbf{s}

$$\mathbf{t}(x_1, x_2) = -\frac{\partial \varphi}{\partial \mathbf{s}}(x_1, x_2), \quad (41)$$

and assuming that the stress function vector φ vanishes at the vertex of the wedge ($r = 0$), a homogeneous and orthogonal boundary condition for an open corner, for a wedge face of angle ϑ_w , $w = 0$ or W , can be imposed by the following linear relation, for $r > 0$,

$$\mathbf{D}_u(\vartheta_w)\mathbf{u}(r, \vartheta_w) + \mathbf{D}_\varphi(\vartheta_w)\varphi(r, \vartheta_w) = \mathbf{0}, \quad (42)$$

where \mathbf{D}_u and \mathbf{D}_φ are 3×3 real matrices which satisfy the orthogonality relations

$$\mathbf{D}_u(\vartheta_w)\mathbf{D}_\varphi^T(\vartheta_w) = \mathbf{D}_\varphi(\vartheta_w)\mathbf{D}_u^T(\vartheta_w) = \mathbf{0}, \quad (43)$$

and

$$\mathbf{D}_u(\vartheta_w)\mathbf{D}_u^T(\vartheta_w) + \mathbf{D}_\varphi(\vartheta_w)\mathbf{D}_\varphi^T(\vartheta_w) = \mathbf{I}, \quad (44)$$

with subscript T denoting the transpose. Examples of these matrices for the most relevant homogeneous and orthogonal boundary conditions are presented in Table 1. It is easy to check that the matrices in Table 1 meet the orthogonality relations (43) and (44), and represent the indicated boundary conditions by applying (42). A reference frame defined by an orthonormal basis of vectors $(\tilde{\mathbf{n}}, \tilde{\mathbf{m}}, \tilde{\mathbf{l}})$ is used to define inclined supports, an example of such reference frame is shown in Fig. 3. Noteworthy, the matrices \mathbf{D}_u and \mathbf{D}_φ are defined in Table 1 in such a way that actually no linear combination of the components of the vectors \mathbf{u} and φ occurs in (42), and the boundary conditions for displacements and stress function vectors are imposed separately.

Matrices \mathbf{D}_u and \mathbf{D}_φ in Table 1 represent just one of many possible options to impose the considered boundary conditions. The presented forms of these matrices have been chosen for convenience due to their simplicity when using the defined reference frames. Nevertheless, there is a lot of freedom when defining these matrices:

- If the displacement vector \mathbf{u} has a null projection onto a straight line, the unite vectors \mathbf{m} and $-\mathbf{m}$, fulfilling $\mathbf{u} \cdot \mathbf{m} = 0$ and $|\mathbf{m}| = 1$, can be used to define that line. Similar consideration can be made for the vector φ .

Table 1

Matrices \mathbf{D}_u and \mathbf{D}_φ for homogeneous and orthogonal boundary conditions.

Boundary condition	\mathbf{D}_u	\mathbf{D}_φ
Free	$\mathbf{0}_3 \times 3$	$\mathbf{I}_3 \times 3$
Clamped	$\mathbf{I}_3 \times 3$	$\mathbf{0}_3 \times 3$
Only u_θ restricted (Symmetry)	$[\mathbf{n}(\vartheta), \mathbf{0}, \mathbf{0}]^T$	$[\mathbf{0}, \mathbf{s}_r(\vartheta), \mathbf{s}_3]^T$
Only u_θ allowed (Antisymmetry)	$[\mathbf{0}, \mathbf{s}_r(\vartheta), \mathbf{s}_3]^T$	$[\mathbf{n}(\vartheta), \mathbf{0}, \mathbf{0}]^T$
Only u_r restricted	$[\mathbf{s}_r(\vartheta), \mathbf{0}, \mathbf{0}]^T$	$[\mathbf{0}, \mathbf{n}(\vartheta), \mathbf{s}_3]^T$
Only u_r allowed	$[\mathbf{n}(\vartheta), \mathbf{s}_3, \mathbf{0}]^T$	$[\mathbf{0}, \mathbf{0}, \mathbf{s}_r(\vartheta)]^T$
Only u_3 restricted	$[\mathbf{s}_3, \mathbf{0}, \mathbf{0}]^T$	$[\mathbf{0}, \mathbf{s}_r(\vartheta), \mathbf{n}(\vartheta)]^T$
Only u_3 allowed	$[\mathbf{s}_r(\vartheta), \mathbf{n}(\vartheta), \mathbf{0}]^T$	$[\mathbf{0}, \mathbf{0}, \mathbf{s}_3]^T$
Only $u_{\tilde{n}}$ restricted	$[\tilde{\mathbf{n}}(\vartheta), \mathbf{0}, \mathbf{0}]^T$	$[\mathbf{0}, \tilde{\mathbf{m}}(\vartheta), \tilde{\mathbf{l}}]^T$
Only $u_{\tilde{n}}$ allowed	$[\tilde{\mathbf{m}}(\vartheta), \tilde{\mathbf{l}}, \mathbf{0}]^T$	$[\mathbf{0}, \mathbf{0}, \tilde{\mathbf{n}}(\vartheta)]^T$

- If the displacement vector \mathbf{u} has a null projection onto a plane, any pair of unit orthogonal vectors \mathbf{m} and \mathbf{l} can be used to define that plane. This pair of vectors fulfills the following relations: $\mathbf{u} \cdot \mathbf{m} = 0$, $\mathbf{u} \cdot \mathbf{l} = 0$, $\mathbf{m} \cdot \mathbf{l} = 0$, $|\mathbf{m}| = |\mathbf{l}| = 1$. Similar consideration can be made for the vector φ .
- Formally, in general, the matrices \mathbf{D}_u and \mathbf{D}_φ presented in Table 1 could be multiplied from the left by any 3×3 real orthogonal matrix. It is easy to check that the matrices obtained by such multiplication will fulfill the orthogonality relations (43) and (44), and will impose the same boundary condition by applying (42). However, such multiplication of \mathbf{D}_u and \mathbf{D}_φ by an orthogonal matrix can lead to a linear combination of the components of \mathbf{u} and φ having different physical units.

With the matrices \mathbf{D}_φ and \mathbf{D}_u we can build the *main matrix for boundary conditions*

$$\mathbf{D}_{BC}(\vartheta_w) = \begin{bmatrix} \mathbf{D}_u(\vartheta_w) & \mathbf{D}_\varphi(\vartheta_w) \\ \tilde{\mathbf{D}}_u(\vartheta_w) & \tilde{\mathbf{D}}_\varphi(\vartheta_w) \end{bmatrix} = \begin{bmatrix} \mathbf{D}_u(\vartheta_w) & \mathbf{D}_\varphi(\vartheta_w) \\ \mathbf{D}_\varphi(\vartheta_w) & \mathbf{D}_u(\vartheta_w) \end{bmatrix}, \quad (45)$$

a 6×6 real matrix that fulfills the orthogonality relation

$$\mathbf{D}_{BC}\mathbf{D}_{BC}^T = \mathbf{D}_{BC}^T\mathbf{D}_{BC} = \mathbf{I}_{6 \times 6}, \quad (46)$$

as follows from the orthogonality relations (43) and (44). Relation (46) is crucial for the procedure devised.

In particular, it can be checked that the matrices \mathbf{D}_φ and \mathbf{D}_u in Table 1 when substituted into (45) verify the orthogonality relation (46).

With this matrix we can get the prescribed and unknown components of $\mathbf{w}(r, \vartheta)$ from expression (30) organized in two separates blocks, only by multiplying the vector $\mathbf{w}(r, \vartheta)$ from the left by the matrix \mathbf{D}_{BC}

$$\mathbf{D}_{BC}\mathbf{w}(r, \vartheta_w) = \begin{bmatrix} \mathbf{w}_p(r, \vartheta_w) \\ \mathbf{w}_U(r, \vartheta_w) \end{bmatrix}, \quad (47)$$

where $\mathbf{w}_p(r, \vartheta_w) = \mathbf{0}$ and $\mathbf{w}_U(r, \vartheta_w)$ are 3×1 vectors in this special case where all the boundary conditions considered are orthogonal.

From the orthogonality relation in (46) and by suppressing the prescribed values $\mathbf{w}_p(r, \vartheta_w)$ we can get the displacement and stress function vectors for $w = 0$ and W

$$\begin{aligned} \mathbf{w}(r, \vartheta_w) &= \mathbf{D}_{BC}^T \begin{bmatrix} \mathbf{w}_p(r, \vartheta_w) \\ \mathbf{w}_U(r, \vartheta_w) \end{bmatrix} = \begin{bmatrix} \mathbf{D}_\varphi^T \\ \mathbf{D}_u^T \end{bmatrix} \mathbf{w}_U(r, \vartheta_w) = \begin{bmatrix} \tilde{\mathbf{D}}_u^T \\ \tilde{\mathbf{D}}_\varphi^T \end{bmatrix} \mathbf{w}_U(r, \vartheta_w) \\ &= \tilde{\mathbf{D}}_{BC}^T \mathbf{w}_U(r, \vartheta_w), \end{aligned} \quad (48)$$

where $\tilde{\mathbf{D}}_{BC}^T$ is a real 6×3 matrix. To facilitate the understanding of this section, an example of how these matrices work is shown in Appendix A. A general matrix formalism closely related to the one described above was introduced by Wu [15], employing the procedure for general boundary conditions in the Stroh formalism developed by Ting and Wang [27,31].

The last two boundary conditions shown in Table 1 represent inclined supports and may need a further explanation. These boundary conditions are restraints with reference to a plane inclined with respect to the contour face, as shown in an example in Fig. 3. In this case, $\tilde{\mathbf{n}}$

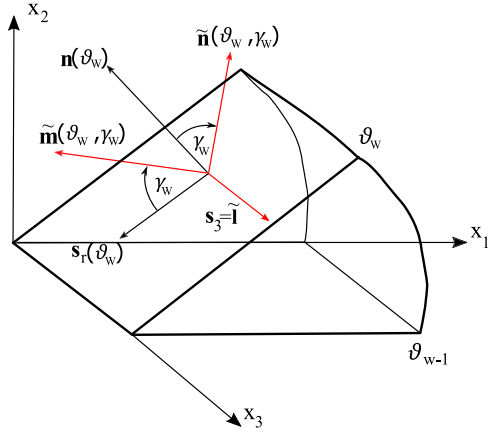


Fig. 3. Reference frame for an inclined plane.

and $\tilde{\mathbf{m}}$, respectively, are the normal and the tangential vector to the inclined plane. Vector $\tilde{\mathbf{I}}$ has the same direction as \mathbf{s}_3 , but it could be not coincident.

The boundary condition *only $\mathbf{u}_{\tilde{\mathbf{n}}}$ restricted* means that displacement in the direction of the vector $\tilde{\mathbf{n}}$ is restricted while it is allowed in the plane given by the vectors $\tilde{\mathbf{m}}$ and $\tilde{\mathbf{I}}$. The boundary condition *only $\mathbf{u}_{\tilde{\mathbf{m}}}$ allowed* means that displacement in the direction of the vector $\tilde{\mathbf{n}}$ is allowed while it is restricted in the plane given by the vectors $\tilde{\mathbf{m}}$ and $\tilde{\mathbf{I}}$. In Section 8.4 an example of application of this kind of boundary conditions is given, showing how γ affects the singularity exponent λ .

4.3. Interface conditions

For both closed and open corners, as long as there are more than one single-material or multi-material wedge, interface conditions should be given between their faces. In the present paper, only homogeneous orthogonal interface conditions, where the stress vector is perpendicular to the relative displacement vector at the interface, are considered, namely: the perfectly bonded and frictionless sliding interface condition. Nevertheless, in the case where two faces of different materials are perfectly bonded, the problem can be significantly simplified by using the *wedge transfer matrix* \mathbf{K}_w , see Section 5.1.

Similarly as for the homogeneous orthogonal boundary conditions, see (42), the homogeneous orthogonal interface conditions can be written in the following form:

$$\mathbf{D}_1(\vartheta_w)\mathbf{w}_w(r, \vartheta_w) + \mathbf{D}_2(\vartheta_w)\mathbf{w}_{w+1}(r, \vartheta_w) = \mathbf{0}, \quad (49)$$

where the real 6×6 matrices \mathbf{D}_1 and \mathbf{D}_2 and the associated matrices $\tilde{\mathbf{D}}_1$ and $\tilde{\mathbf{D}}_2$ satisfy the following orthogonality relations:

$$\begin{aligned} \mathbf{D}_1\mathbf{D}_1^T + \mathbf{D}_2\mathbf{D}_2^T &= \mathbf{I}_{6 \times 6}, \\ \tilde{\mathbf{D}}_1\tilde{\mathbf{D}}_1^T + \tilde{\mathbf{D}}_2\tilde{\mathbf{D}}_2^T &= \mathbf{I}_{6 \times 6}, \\ \mathbf{D}_1\tilde{\mathbf{D}}_1^T + \mathbf{D}_2\tilde{\mathbf{D}}_2^T &= \mathbf{0}_{6 \times 6}. \end{aligned} \quad (50)$$

Typical examples of the real 6×6 matrices \mathbf{D}_1 , \mathbf{D}_2 , $\tilde{\mathbf{D}}_1$ and $\tilde{\mathbf{D}}_2$ are shown in Table 2. Matrices for *perfectly bonded interface* will be barely used, mostly for the purpose of code testing. The reason for this is explained in Section 5.1. The coefficients $\sqrt{2}$ and $\frac{1}{\sqrt{2}}$ are used to fulfill the orthogonality relationship. These matrices represent just one of many possible options to impose the considered interface conditions. Formally, in general, the matrices presented in Table 2 could be multiplied from the left by any 6×6 real orthogonal matrix. It is easy to check that the matrices obtained by such multiplication will fulfill the orthogonality relations (50) and will impose the same interface condition by applying (49). However, such multiplication of \mathbf{D}_1 and \mathbf{D}_2 by an orthogonal matrix can lead to a linear combination of the

components of the displacement and stress function vectors on the wedge interface having different physical units.

The *main matrix for interface conditions* is defined as a real 12×12 matrix, analogous to the matrix \mathbf{D}_{BC} defined in (45):

$$\mathbf{D}_I(\vartheta_w) = \begin{bmatrix} \mathbf{D}_1(\vartheta_w) & \mathbf{D}_2(\vartheta_w) \\ \tilde{\mathbf{D}}_1(\vartheta_w) & \tilde{\mathbf{D}}_2(\vartheta_w) \end{bmatrix}. \quad (51)$$

From the orthogonality relations (50), the matrix \mathbf{D}_I fulfills the following orthogonality relation, similar to (46) for \mathbf{D}_{BC} :

$$\mathbf{D}_I\mathbf{D}_I^T = \mathbf{D}_I^T\mathbf{D}_I = \mathbf{I}_{12 \times 12}. \quad (52)$$

Following the same process as for boundary conditions, if we multiply the matrix \mathbf{D}_I from the right by the 12×1 vector $(\mathbf{w}_w^T(r, \vartheta_w), \mathbf{w}_{w+1}^T(r, \vartheta_w))^T$, we get a vector in which we can separate the prescribed from the unknown components, $\mathbf{w}_P(r, \vartheta_w)$ and $\mathbf{w}_U(r, \vartheta_w)$, respectively,

$$\mathbf{D}_I \begin{bmatrix} \mathbf{w}_w(r, \vartheta_w) \\ \mathbf{w}_{w+1}(r, \vartheta_w) \end{bmatrix} = \begin{bmatrix} \mathbf{w}_P(r, \vartheta_w) \\ \mathbf{w}_U(r, \vartheta_w) \end{bmatrix}. \quad (53)$$

From the orthogonality relation (52) and knowing that $\mathbf{w}_P(r, \vartheta_w) = \mathbf{0}$ we can get the displacement and stress function vectors for $1 \leq w \leq W - 1$

$$\begin{bmatrix} \mathbf{w}_w(r, \vartheta_w) \\ \mathbf{w}_{w+1}(r, \vartheta_w) \end{bmatrix} = \mathbf{D}_I^T \begin{bmatrix} \mathbf{w}_P(r, \vartheta_w) \\ \mathbf{w}_U(r, \vartheta_w) \end{bmatrix} = \begin{bmatrix} \tilde{\mathbf{D}}_1^T \\ \tilde{\mathbf{D}}_2^T \end{bmatrix} \mathbf{w}_U(r, \vartheta_w). \quad (54)$$

In Appendix B, an example of how these matrices for interface conditions work can be found.

5. Characteristic system for the analysis of singularities in a multi-material elastic corner

Once the matrices for the material wedges and for the boundary and interface conditions are available, the *characteristic matrix of the corner* is assembled. The assembly of this matrix will depend on whether the corner is open or closed (periodic corner).

Initially, regardless the case, the size of this matrix would be $6M \times 6M$, M being the number of single-material wedges (materials). As it will be stated in Section 5.3, to solve the corner problem, the determinant of this matrix should be numerically solved. Computational complexity of the determinant evaluation increases with the matrix size as $O(n^3)$ if it is solved numerically, where n is the number of columns or rows of the matrix. This means, if we have 3 materials, to solve the determinant we will need about $(6M)^3 = (6 * 3)^3 = 5832$ operations while if the corner is made by 5 materials, we will need about $(6M)^3 = (6 * 5)^3 = 27000$ operations. This can be simplified if some of those materials are perfectly bonded by making use of the *multi-material-wedge transfer matrix*.

5.1. Multi-material-wedge transfer matrix

To explain the deduction of the transfer matrix for a multi-material wedge, we will use a simple example of a wedge given by three materials perfectly bonded. Let us call these materials as M_1 , M_2 and M_3 . On the perfectly bonded interfaces at the angles θ_m between M_m and M_{m+1} ($m = 1, 2$), the displacements given in bonded points on both sides of the interface are identical and tractions at those points are in equilibrium, which can be expressed as

$$\mathbf{w}_m(r, \theta_m) = \mathbf{w}_{m+1}(r, \theta_m). \quad (55)$$

Then, as it was shown in (32), the *transfer matrix* of a single-material wedge relates displacements and tractions on both faces considering a power law elastic solution. We will see now that it is possible to extend this relation to a *multi-material wedge*. Getting back to the above three-material wedge, we can follow this chain of relations until to get the *multi-material-wedge transfer matrix*, see equation given in Box 1,

Table 2
Matrices \mathbf{D}_1 , \mathbf{D}_2 , $\tilde{\mathbf{D}}_1$ and $\tilde{\mathbf{D}}_2$ for interface conditions.

Perfectly bonded interface	$\mathbf{D}_1(\vartheta) = -\frac{1}{\sqrt{2}}\mathbf{I}_{6 \times 6}$ $\tilde{\mathbf{D}}_1(\vartheta) = \frac{1}{\sqrt{2}}\mathbf{I}_{6 \times 6}$	$\mathbf{D}_2(\vartheta) = \frac{1}{\sqrt{2}}\mathbf{I}_{6 \times 6}$ $\tilde{\mathbf{D}}_2(\vartheta) = \frac{1}{\sqrt{2}}\mathbf{I}_{6 \times 6}$
Frictionless interface	$\mathbf{D}_1(\vartheta) = \frac{1}{\sqrt{2}} \begin{bmatrix} -\mathbf{n}(\vartheta) & \mathbf{0}_{3 \times 1} & \mathbf{0}_{3 \times 3} & \mathbf{0}_{3 \times 1} \\ \mathbf{0}_{3 \times 1} & \mathbf{s}_r(\vartheta) & -\mathbf{I}_{3 \times 3} & \mathbf{s}_3 \end{bmatrix}^T$	
	$\mathbf{D}_2(\vartheta) = \frac{1}{\sqrt{2}} \begin{bmatrix} \mathbf{n}(\vartheta) & \mathbf{0}_{3 \times 1} & \mathbf{0}_{3 \times 3} & \mathbf{0}_{3 \times 1} \\ \mathbf{0}_{3 \times 1} & \mathbf{s}_r(\vartheta) & \mathbf{I}_{3 \times 3} & \mathbf{s}_3 \end{bmatrix}^T$	
	$\tilde{\mathbf{D}}_1(\vartheta) = \frac{1}{\sqrt{2}} \begin{bmatrix} \mathbf{n}(\vartheta) & \mathbf{0}_{3 \times 1} & \sqrt{2}\mathbf{s}_r(\vartheta) & \mathbf{0}_{3 \times 1} & \sqrt{2}\mathbf{s}_3 & \mathbf{0}_{3 \times 1} \\ \mathbf{0}_{3 \times 1} & \mathbf{n}(\vartheta) & \mathbf{0}_{3 \times 1} & \mathbf{0}_{3 \times 1} & \mathbf{0}_{3 \times 1} & \mathbf{0}_{3 \times 1} \end{bmatrix}^T$	
	$\tilde{\mathbf{D}}_2(\vartheta) = \frac{1}{\sqrt{2}} \begin{bmatrix} \mathbf{n}(\vartheta) & \mathbf{0}_{3 \times 1} & \mathbf{0}_{3 \times 1} & \sqrt{2}\mathbf{s}_r(\vartheta) & \mathbf{0}_{3 \times 1} & \sqrt{2}\mathbf{s}_3 \\ \mathbf{0}_{3 \times 1} & \mathbf{n}(\vartheta) & \mathbf{0}_{3 \times 1} & \mathbf{0}_{3 \times 1} & \mathbf{0}_{3 \times 1} & \mathbf{0}_{3 \times 1} \end{bmatrix}^T$	

$$\begin{array}{c}
 \mathbf{w}_3(r, \vartheta_3) = \mathbf{E}_3(\lambda)\mathbf{w}_3(r, \vartheta_2) \\
 \mathbf{w}_3(r, \vartheta_2) = \mathbf{w}_2(r, \vartheta_2)
 \end{array}
 \left|
 \begin{array}{c}
 \mathbf{w}_3(r, \vartheta_3) = \mathbf{E}_3(\lambda)\mathbf{w}_2(r, \vartheta_2) \\
 \mathbf{w}_2(r, \vartheta_2) = \mathbf{E}_2(\lambda)\mathbf{w}_2(r, \vartheta_1)
 \end{array}
 \right|
 \begin{array}{c}
 \mathbf{w}_3(r, \vartheta_3) = \mathbf{E}_3(\lambda)\mathbf{E}_2(\lambda)\mathbf{w}_2(r, \vartheta_1) \\
 \mathbf{w}_2(r, \vartheta_1) = \mathbf{w}_1(r, \vartheta_1)
 \end{array}
 \left|
 \begin{array}{c}
 \mathbf{w}_3(r, \vartheta_3) = \mathbf{E}_3(\lambda)\mathbf{E}_2(\lambda)\mathbf{w}_1(r, \vartheta_1) \\
 \mathbf{w}_1(r, \vartheta_1) = \mathbf{E}_1(\lambda)\mathbf{w}_1(r, \vartheta_0)
 \end{array}
 \right|$$

Box I.

and finally

$$\mathbf{w}_3(r, \vartheta_3) = \mathbf{E}_3(\lambda)\mathbf{E}_2(\lambda)\mathbf{E}_1(\lambda)\mathbf{w}_1(r, \vartheta_0). \tag{56}$$

By introducing the *three-material-wedge transfer matrix*

$$\mathbf{K}_1(\lambda) = \mathbf{E}_3(\lambda)\mathbf{E}_2(\lambda)\mathbf{E}_1(\lambda), \tag{57}$$

and changing from material notation to multi-material wedge notation, relation (56) can be written as

$$\mathbf{w}_1(r, \vartheta_1) = \mathbf{K}_1(\lambda)\mathbf{w}_1(r, \vartheta_0). \tag{58}$$

We can write this expression in a generic way as:

$$\mathbf{w}_w(r, \vartheta_w) = \mathbf{K}_w(\lambda)\mathbf{w}_w(r, \vartheta_{w-1}). \tag{59}$$

This is the *transfer relation for the wedge w* proposed by Ting [24], relating the elastic variables between the external faces of a wedge considering a power law elastic solution, where the matrix $\mathbf{K}_w(\lambda)$ is given as

$$\mathbf{K}_w(\lambda) = \mathbf{E}_{j_w}(\lambda) \cdot \mathbf{E}_{j_{w-1}}(\lambda) \dots \mathbf{E}_{i_{w+1}}(\lambda) \cdot \mathbf{E}_{i_w}(\lambda). \tag{60}$$

This is a 6×6 complex-valued matrix, no matter the number of materials that conform the multi-material wedge with perfectly bonded interfaces.

This simplification helps to reduce computing time, because now the size of the matrix determinant to solve is $6W \times 6W$ instead of $6M \times 6M$. This means that to solve numerically the determinant of a *characteristic matrix* of a three perfectly bonded materials wedge, we go from $(6 \times 3)^3 = 5832$ operations to $(6 \times 1)^3 = 216$ operations, considerably reducing the computing time.

The assembly of the characteristic system of a multi-material corner will be based on the *transfer relation for a wedge* (59) rewritten as

$$[\mathbf{K}_w(\lambda) - \mathbf{I}_{6 \times 6}] \begin{bmatrix} \mathbf{w}_w(r, \vartheta_{w-1}) \\ \mathbf{w}_w(r, \vartheta_w) \end{bmatrix} = \mathbf{0}_{6 \times 1}, \tag{61}$$

where the first matrix on the left hand side is a rectangular 6×12 matrix.

5.2. Characteristic system assembly for a multi-material corner

If in a corner, one or several interfaces are not perfectly bonded, there are more than one wedge in such corner. In this case, we

can gather all the multi-material-wedge transfer matrices $\mathbf{K}_w(\lambda)$ in a $6W \times 12W$ extended complex matrix of transfer relations of the multi-material corner

$$\mathbf{K}_{\text{corner_ext.}}(\lambda) = \begin{bmatrix} \mathbf{K}_1(\lambda) & -\mathbf{I}_{6 \times 6} & \mathbf{0}_{6 \times 6} & \mathbf{0}_{6 \times 6} & \dots & \dots & \mathbf{0}_{6 \times 6} \\ \mathbf{0}_{6 \times 6} & \mathbf{0}_{6 \times 6} & \mathbf{K}_2(\lambda) & -\mathbf{I}_{6 \times 6} & \dots & \dots & \mathbf{0}_{6 \times 6} \\ \vdots & \vdots & \vdots & \vdots & \ddots & \vdots & \vdots \\ \mathbf{0}_{6 \times 6} & \mathbf{0}_{6 \times 6} & \mathbf{0}_{6 \times 6} & \mathbf{0}_{6 \times 6} & \dots & \mathbf{K}_W(\lambda) & -\mathbf{I}_{6 \times 6} \end{bmatrix}, \tag{62}$$

and also gather all the elastic variable vectors $\mathbf{w}_w(r, \vartheta_w)$ and $\mathbf{w}_w(r, \vartheta_{w-1})$ in a $12W \times 1$ vector of elastic variables (displacement and stress function vectors) at all wedge faces

$$\mathbf{w}_{\text{corner_ext.}} = \begin{bmatrix} \mathbf{w}_1(r, \vartheta_0) \\ \mathbf{w}_1(r, \vartheta_1) \\ \mathbf{w}_2(r, \vartheta_1) \\ \mathbf{w}_2(r, \vartheta_2) \\ \vdots \\ \mathbf{w}_W(r, \vartheta_{W-1}) \\ \mathbf{w}_W(r, \vartheta_W) \end{bmatrix}. \tag{63}$$

All the wedge transfer relations for wedges $w = 1, \dots, W$ in (61) can be written in a compact form as

$$\mathbf{K}_{\text{corner_ext.}}(\lambda)\mathbf{w}_{\text{corner_ext.}} = \mathbf{0}_{6W \times 1}. \tag{64}$$

Recall, that the complex-valued matrix $\mathbf{K}_{\text{corner_ext.}}(\lambda)$ depends, in addition to λ , also on the material properties and the polar angles of all single-material wedges in the corner.

With the aim to assemble the characteristic system for an open corner by matrix multiplication, we need to gather all boundary and interface condition matrices in a suitable way, fitting the structure of the matrix $\mathbf{K}_{\text{corner_ext.}}(\lambda)$. This will be done in Sections 5.2.1 and 5.2.2 by gathering the matrices \mathbf{D}_{BC} and \mathbf{D}_1 of the corner to form the so-called *extended boundary and interface condition matrix* $\mathbf{D}_{\text{corner_ext.}}(\vartheta)$. Considering that the matrices $\mathbf{D}_{\text{BC}}(\vartheta_w)$ and $\mathbf{D}_1(\vartheta_w)$ fulfill the orthogonality relations in (46) and (52), we can prove that the matrix $\mathbf{D}_{\text{corner_ext.}}(\vartheta)$ fulfills the following orthogonality relation

$$\mathbf{D}_{\text{corner_ext.}}(\vartheta)\mathbf{D}_{\text{corner_ext.}}^T(\vartheta) = \mathbf{I}_{12W \times 12W}, \tag{65}$$

where

$$\vartheta = (\vartheta_0, \vartheta_1, \dots, \vartheta_W). \tag{66}$$

5.2.1. Open corner

Extended boundary and interface condition matrix. In the case of an open corner, the boundary and interface condition matrices, defined in Sections 4.2 and 4.3, are assembled in a real-valued $12W \times 12W$ extended matrix of boundary and interface conditions for an open multi-material corner

$$\mathbf{D}_{\text{corner_ext.}}(\boldsymbol{\theta}) = \text{blocked_diag}[\mathbf{D}_{\text{BC}}(\vartheta_0), \mathbf{D}_{\text{I}}(\vartheta_1), \dots, \mathbf{D}_{\text{BC}}(\vartheta_W)]$$

$$= \begin{bmatrix} \mathbf{D}_{\text{BC}}(\vartheta_0) & \mathbf{0}_{6 \times 12} & \mathbf{0}_{6 \times 12} & \cdots & \mathbf{0}_{6 \times 6} \\ \mathbf{0}_{12 \times 6} & \mathbf{D}_{\text{I}}(\vartheta_1) & \mathbf{0}_{12 \times 12} & \cdots & \mathbf{0}_{12 \times 6} \\ \vdots & \vdots & \vdots & \ddots & \vdots \\ \mathbf{0}_{6 \times 6} & \mathbf{0}_{6 \times 12} & \mathbf{0}_{6 \times 12} & \cdots & \mathbf{D}_{\text{BC}}(\vartheta_W) \end{bmatrix}. \quad (67)$$

Recall that \mathbf{D}_{BC} and \mathbf{D}_{I} are 6×6 and 12×12 matrices, respectively. It is easy to prove that this matrix satisfies the orthogonality relation (65), as it is a block diagonal matrix whose main-diagonal block matrices $\mathbf{D}_{\text{BC}}(\vartheta_0)$, $\mathbf{D}_{\text{I}}(\vartheta_1)$, ... and $\mathbf{D}_{\text{BC}}(\vartheta_W)$ are orthogonal.

Open corner characteristic matrix. As previously done for an elastic variable vector $\mathbf{w}_w(r, \vartheta_w)$ for a wedge w in expression (47), when multiplying the matrix $\mathbf{D}_{\text{corner_ext.}}$ by the $\mathbf{w}_{\text{corner_ext.}}$ vector, we get the $\mathbf{w}_{\text{corner_PU}}$ which can be partitioned into sub-vectors of the prescribed and unknown variables

$$\mathbf{D}_{\text{corner_ext.}}(\boldsymbol{\theta})\mathbf{w}_{\text{corner_ext.}} = \mathbf{w}_{\text{corner_PU}}. \quad (68)$$

where the $12W \times 1$ vector

$$\mathbf{w}_{\text{corner_PU}} = \begin{bmatrix} \mathbf{w}_p(r, \vartheta_0) \\ \mathbf{w}_u(r, \vartheta_0) \\ \mathbf{w}_p(r, \vartheta_1) \\ \mathbf{w}_u(r, \vartheta_1) \\ \vdots \\ \mathbf{w}_p(r, \vartheta_W) \\ \mathbf{w}_u(r, \vartheta_W) \end{bmatrix}, \quad (69)$$

can be reduced to the $6W \times 1$ vector of unknown variables, considering that the prescribed variables vanish,

$$\mathbf{w}_{\text{corner_U}} = \begin{bmatrix} \mathbf{w}_u(r, \vartheta_0) \\ \mathbf{w}_u(r, \vartheta_1) \\ \vdots \\ \mathbf{w}_u(r, \vartheta_W) \end{bmatrix}. \quad (70)$$

Note that the vectors $\mathbf{w}_u(r, \vartheta_w)$ for ϑ_0 and ϑ_W are 3×1 vectors, as they are the unknown variables for displacement and stress function vectors on the boundaries, while for the interfaces at $\vartheta_1, \dots, \vartheta_{W-1}$ they are 6×1 vectors.

In view of the orthogonality property (65), relation (68) can be rewritten as

$$\mathbf{w}_{\text{corner_ext.}} = \mathbf{D}_{\text{corner_ext.}}^T(\boldsymbol{\theta})\mathbf{w}_{\text{corner_PU}}. \quad (71)$$

which substituted into (64) leads to

$$\mathbf{K}_{\text{corner_ext.}}(\lambda)\mathbf{D}_{\text{corner_ext.}}^T(\boldsymbol{\theta})\mathbf{w}_{\text{corner_PU}} = \mathbf{0}_{6W \times 1}. \quad (72)$$

In this expression, some columns of the matrix obtained by multiplying $\mathbf{K}_{\text{corner_ext.}}(\lambda)$ by $\mathbf{D}_{\text{corner_ext.}}^T(\boldsymbol{\theta})$ can be removed as they would be multiplied by the prescribed zero values of $\mathbf{w}_p(r, \vartheta_w)$. This procedure leads to the final complex-valued square matrix with the reduced dimensions ($6W \times 6W$)

$$\mathbf{K}_{\text{corner}}(\lambda) = \begin{bmatrix} \mathbf{K}_1 \tilde{\mathbf{D}}_{\text{BC}}^T(\vartheta_0) & -\tilde{\mathbf{D}}_1^T(\vartheta_1) & \mathbf{0}_{6 \times 6} & \cdots & \mathbf{0}_{6 \times 6} & \mathbf{0}_{6 \times 3} \\ \mathbf{0}_{6 \times 3} & \mathbf{K}_2 \tilde{\mathbf{D}}_2^T(\vartheta_1) & -\tilde{\mathbf{D}}_1^T(\vartheta_2) & \cdots & \mathbf{0}_{6 \times 6} & \mathbf{0}_{6 \times 3} \\ \vdots & \vdots & \vdots & \ddots & \vdots & \vdots \\ \mathbf{0}_{6 \times 3} & \mathbf{0}_{6 \times 6} & \mathbf{0}_{6 \times 6} & \cdots & \mathbf{K}_W \tilde{\mathbf{D}}_2^T(\vartheta_{W-1}) & -\tilde{\mathbf{D}}_{\text{BC}}^T(\vartheta_W) \end{bmatrix}, \quad (73)$$

which introduced into (72) together with (70) gives the characteristic system for the singularity analysis of an open multi-material corner, which represents a nonlinear eigenvalue problem for this corner,

$$\mathbf{K}_{\text{corner}}(\lambda)\mathbf{w}_{\text{corner_U}} = \mathbf{0}_{6W \times 1}. \quad (74)$$

Examples of open corners composed by three wedges, i.e. $W = 3$, are studied in Table 9. As it may be not so easily inferred from the general structure of $\mathbf{K}_{\text{corner}}(\lambda)$ in (73) which is the structure of this matrix for a particular case of a corner with a small number of wedges $W = 1$ or 2, these cases will be described in detail in the following.

One-wedge corner. In the case of one wedge, $W = 1$, $\mathbf{K}_{\text{corner}}(\lambda)$ is a 6×6 matrix defined as

$$\mathbf{K}_{\text{corner}}(\lambda) = [\mathbf{K}_1(\lambda)\tilde{\mathbf{D}}_{\text{BC}}^T(\vartheta_0) \quad -\tilde{\mathbf{D}}_{\text{BC}}^T(\vartheta_1)], \quad (75)$$

where $\tilde{\mathbf{D}}_{\text{BC}}^T(\vartheta_w)$, for $w = 0$ and 1, are real 6×3 matrices, see (48).

Actually, in the cases studied in the present work, where only orthogonal boundary conditions can be prescribed on both boundary surfaces, this can be even further reduced, cf. [15,20,32],

$$\mathbf{K}_{\text{corner_reduced}}(\lambda) = \mathbf{D}_u(\vartheta_1)\mathbf{K}_1^{(1)}(\lambda)\tilde{\mathbf{D}}_u^T(\vartheta_0) + \mathbf{D}_u(\vartheta_1)\mathbf{K}_1^{(2)}(\lambda)\tilde{\mathbf{D}}_\varphi^T(\vartheta_0) + \mathbf{D}_\varphi(\vartheta_1)\mathbf{K}_1^{(3)}(\lambda)\tilde{\mathbf{D}}_u^T(\vartheta_0) + \mathbf{D}_\varphi(\vartheta_1)\mathbf{K}_1^{(4)}(\lambda)\tilde{\mathbf{D}}_\varphi^T(\vartheta_0), \quad (76)$$

where $\mathbf{K}_1^{(i)}$ are the 3×3 sub-matrices that form the 6×6 wedge transfer matrix of the first and only wedge in this kind of corners

$$\mathbf{K}_1(\lambda) = \begin{bmatrix} \mathbf{K}_1^{(1)}(\lambda) & \mathbf{K}_1^{(2)}(\lambda) \\ \mathbf{K}_1^{(3)}(\lambda) & \mathbf{K}_1^{(4)}(\lambda) \end{bmatrix}. \quad (77)$$

The characteristic system in this case reduces to

$$\mathbf{K}_{\text{corner_reduced}}(\lambda)\mathbf{w}_{\text{corner_U}}(r, \vartheta_0) = \mathbf{0}_{3 \times 1}. \quad (78)$$

Results of singularity analysis for several examples of this kind of corners can be found in Tables 4–7.

Two-wedge corner. For the corners composed by two wedges, $W = 2$, the structure of the 12×12 corner characteristic matrix is

$$\mathbf{K}_{\text{corner}}(\lambda) = \begin{bmatrix} \mathbf{K}_1 \tilde{\mathbf{D}}_{\text{BC}}^T(\vartheta_0) & -\tilde{\mathbf{D}}_1^T(\vartheta_1) & \mathbf{0}_{6 \times 3} \\ \mathbf{0}_{6 \times 3} & \mathbf{K}_2 \tilde{\mathbf{D}}_2^T(\vartheta_1) & -\tilde{\mathbf{D}}_{\text{BC}}^T(\vartheta_2) \end{bmatrix}. \quad (79)$$

Results of singularity analysis for several examples of two wedge corners can be found in Table 8.

5.2.2. Closed corner (periodic corner)

Extended interface condition matrix. The procedure to obtain the characteristic matrix of the corner is similar to the one presented in Section 5.2.1, but in contrast with open corners, in closed corners there are no boundary conditions and only interface conditions are prescribed. For this reason the extended matrix of interface conditions for a closed multi-material corner is different from that for an open corner. The structure of this matrix for closed corners, defined by all the interface condition matrices, is somewhat more involved than for open corners,

$$\mathbf{D}_{\text{corner_ext.}}(\boldsymbol{\theta}) = \begin{bmatrix} \mathbf{D}_2(\vartheta_0) & \mathbf{0}_{6 \times 12} & \mathbf{0}_{6 \times 12} & \cdots & \mathbf{0}_{6 \times 12} & \mathbf{D}_1(\vartheta_W) \\ \tilde{\mathbf{D}}_2(\vartheta_0) & \mathbf{0}_{6 \times 12} & \mathbf{0}_{6 \times 12} & \cdots & \mathbf{0}_{6 \times 12} & \tilde{\mathbf{D}}_1(\vartheta_W) \\ \mathbf{0}_{12 \times 6} & \mathbf{D}_1(\vartheta_1) & \mathbf{0}_{12 \times 12} & \cdots & \mathbf{0}_{12 \times 12} & \mathbf{0}_{12 \times 6} \\ \vdots & \vdots & \vdots & \ddots & \vdots & \vdots \\ \mathbf{0}_{12 \times 6} & \mathbf{0}_{12 \times 12} & \mathbf{0}_{12 \times 12} & \cdots & \mathbf{D}_1(\vartheta_{W-1}) & \mathbf{0}_{12 \times 6} \end{bmatrix}. \quad (80)$$

This is a $12W \times 12W$ real-valued matrix constructed in such a way that it fulfills the orthogonality condition (65), as shown in Appendix C. Remember that, as it is a closed corner, its first and last angle must meet the following relation: $\vartheta_W = \vartheta_0 + 360^\circ$.

$$\mathbf{K}_{\text{corner}}(\lambda) = \begin{bmatrix} \mathbf{K}_1 \tilde{\mathbf{D}}_2^T(\vartheta_0) & -\tilde{\mathbf{D}}_1^T(\vartheta_1) & \mathbf{0}_{6 \times 6} & \cdots & \mathbf{0}_{6 \times 6} & \mathbf{0}_{6 \times 6} \\ \mathbf{0}_{6 \times 6} & \mathbf{K}_2 \tilde{\mathbf{D}}_2^T(\vartheta_1) & -\tilde{\mathbf{D}}_1^T(\vartheta_2) & \cdots & \mathbf{0}_{6 \times 6} & \mathbf{0}_{6 \times 6} \\ \vdots & \vdots & \vdots & \ddots & \vdots & \vdots \\ \mathbf{0}_{6 \times 6} & \mathbf{0}_{6 \times 6} & \mathbf{0}_{6 \times 6} & \cdots & \mathbf{K}_{W-1} \tilde{\mathbf{D}}_2^T(\vartheta_{W-2}) & -\tilde{\mathbf{D}}_1^T(\vartheta_{W-1}) \\ -\tilde{\mathbf{D}}_1^T(\vartheta_0) & \mathbf{0}_{6 \times 6} & \mathbf{0}_{6 \times 6} & \cdots & \mathbf{0}_{6 \times 6} & \mathbf{K}_W \tilde{\mathbf{D}}_2^T(\vartheta_{W-1}) \end{bmatrix}, \quad (86)$$

Box II.

Closed corner characteristic matrix. As for an open corner, when multiplying the matrix $\mathbf{D}_{\text{corner_ext}}$ by the $\mathbf{w}_{\text{corner_ext}}$ vector, we get the $12W \times 1$ vector $\mathbf{w}_{\text{corner_PU}}$

$$\mathbf{w}_{\text{corner_PU}} = \mathbf{D}_{\text{corner_ext}}(\vartheta) \mathbf{w}_{\text{corner_ext}}. \quad (81)$$

This vector can be partitioned in sub-vectors of the prescribed and unknown variables on interfaces

$$\mathbf{w}_{\text{corner_PU}} = \begin{bmatrix} \mathbf{w}_P(r, \vartheta_0) \\ \mathbf{w}_U(r, \vartheta_0) \\ \mathbf{w}_P(r, \vartheta_1) \\ \mathbf{w}_U(r, \vartheta_1) \\ \vdots \\ \mathbf{w}_P(r, \vartheta_{W-1}) \\ \mathbf{w}_U(r, \vartheta_{W-1}) \end{bmatrix}. \quad (82)$$

By omitting the prescribed variables in $\mathbf{w}_{\text{corner_PU}}$, the following $6W \times 1$ vector $\mathbf{w}_{\text{corner_U}}$ of unknown variables is obtained:

$$\mathbf{w}_{\text{corner_U}} = \begin{bmatrix} \mathbf{w}_U(r, \vartheta_0) \\ \mathbf{w}_U(r, \vartheta_1) \\ \vdots \\ \mathbf{w}_U(r, \vartheta_{W-1}) \end{bmatrix}. \quad (83)$$

For closed corners, all the subvectors $\mathbf{w}_U(r, \vartheta_w)$ are 6×1 vectors. In view of the orthogonality relation (65), Eq. (81) can be rewritten as

$$\mathbf{w}_{\text{corner_ext}} = \mathbf{D}_{\text{corner_ext}}^T(\vartheta) \mathbf{w}_{\text{corner_PU}}. \quad (84)$$

Then, by substituting this equation in (64) we obtain

$$\mathbf{K}_{\text{corner_ext}}(\lambda) \mathbf{D}_{\text{corner_ext}}^T(\vartheta) \mathbf{w}_{\text{corner_PU}} = \mathbf{0}_{6W \times 1}. \quad (85)$$

In this expression some columns of the matrix given by multiplying $\mathbf{K}_{\text{corner_ext}}(\lambda)$ by $\mathbf{D}_{\text{corner_ext}}^T(\vartheta)$ can be removed as they would be multiplied by the prescribed zero values of $\mathbf{w}_P(r, \vartheta_w)$. This leads to a reduced $6W \times 6W$ complex-valued matrix in Eq. (86), shown in Box II, whose application in (85) together with (83) leads to the *characteristic system for the singularity analysis of a closed multi-material corner*, which represents a nonlinear eigenvalue problem for this corner,

$$\mathbf{K}_{\text{corner}}(\lambda) \mathbf{w}_{\text{corner_U}} = \mathbf{0}_{6W \times 1}. \quad (87)$$

Examples of closed corners composed by more than one wedge, i.e. $W \geq 2$, are studied in Table 11. Similarly as for open corners, it may be not an easy task to infer from the general structure described in (86) the structure of $\mathbf{K}_{\text{corner}}(\lambda)$ for the cases with only one wedge, i.e. $W = 1$. Therefore, these special cases will be studied in detail in the following.

One-wedge corner. Two cases can be considered in closed corners with only one wedge, i.e. $W = 1$. The first case with all the materials perfectly bonded, and the second case with frictionless sliding on one of the interfaces.

In the first case, as there is no boundary condition, $\mathbf{K}_{\text{corner}}$ can be calculated as

$$\mathbf{K}_{\text{corner}}(\lambda) = \mathbf{K}_1 - \mathbf{I}_{6 \times 6}. \quad (88)$$

This kind of corners is studied in Examples 3.1, 3.2 and 3.4 in Table 10. It is easy to see that in this case, singularity exponents in the range

$0 < \text{Re} \lambda < 1$ may only exist when there are two or more dissimilar materials perfectly bonded, i.e. $M \geq 2$. In case that the corner is made by a single material, then $\lambda = n$, where n is an integer number.

In the second case, when the corner is made by one single-material or multi-material wedge and one of its interface conditions is frictionless sliding contact (here considered at ϑ_0), $\mathbf{K}_{\text{corner}}$ can be calculated as follows

$$\mathbf{K}_{\text{corner_ext}}(\lambda) \mathbf{D}_{\text{corner_ext}}^T(\vartheta_0) \mathbf{w}_{\text{corner_PU}}(r, \vartheta_0) = \mathbf{0}_{6 \times 1}, \quad (89)$$

$$[\mathbf{K}_1(\lambda) \quad -\mathbf{I}_{6 \times 6}] \begin{bmatrix} \mathbf{D}_2^T(\vartheta_0) & \tilde{\mathbf{D}}_2^T(\vartheta_0) \\ \mathbf{D}_1^T(\vartheta_1) & \tilde{\mathbf{D}}_1^T(\vartheta_1) \end{bmatrix} \begin{bmatrix} \mathbf{0} \\ \mathbf{w}_{\text{corner_U}}(r, \vartheta_0) \end{bmatrix} = \mathbf{0}, \quad (90)$$

$$[\mathbf{K}_1(\lambda) \mathbf{D}_2^T(\vartheta_0) - \mathbf{D}_1^T(\vartheta_1) \quad \mathbf{K}_1(\lambda) \tilde{\mathbf{D}}_2^T(\vartheta_0) - \tilde{\mathbf{D}}_1^T(\vartheta_1)] \begin{bmatrix} \mathbf{0} \\ \mathbf{w}_{\text{corner_U}}(r, \vartheta_0) \end{bmatrix} = \mathbf{0}, \quad (91)$$

$$[\mathbf{K}_1(\lambda) \tilde{\mathbf{D}}_2^T(\vartheta_0) - \tilde{\mathbf{D}}_1^T(\vartheta_1)] \mathbf{w}_{\text{corner_U}}(r, \vartheta_0) = \mathbf{0}, \quad (92)$$

$$\mathbf{K}_{\text{corner}}(\lambda) = \mathbf{K}_1 \tilde{\mathbf{D}}_2^T(\vartheta_0) - \tilde{\mathbf{D}}_1^T(\vartheta_1). \quad (93)$$

Recall that $\vartheta_1 = \vartheta_0 + 360^\circ$. These kind of corners are studied in Examples 3.3, 3.5 and 3.6 in Table 10. In the special case with the wedge given by a single material, $\lambda = 0.5 + n$, where n is an integer number.

5.3. Solution of the characteristic system. Singular elastic solution

Avoiding the trivial solution for $\mathbf{w}_{\text{corner_U}}$, where $\mathbf{w}_{\text{corner_U}} = \mathbf{0}$, any other solution of the corner eigenequation, (74) for open corners and (87) for closed corners, is a (right) null vector of the corner characteristic matrix $\mathbf{K}_{\text{corner}}(\lambda)$. To get to this solution, we need first to find the *characteristic (singular) values of λ* , for which the complex-valued matrix $\mathbf{K}_{\text{corner}}(\lambda)$ is singular with null determinant. Therefore, a straightforward method to find the singular values is finding the roots of the matrix determinant

$$\det \mathbf{K}_{\text{corner}}(\lambda) = 0. \quad (94)$$

Up to this point, all the steps of the present procedure have been analytical except for the procedure for computing the roots of the Lekhnitskii–Stroh sextic characteristic polynomial of an anisotropic linear elastic material in those cases where its roots cannot be expressed in terms of radicals [33,34]. In some specific cases, this sextic equation can be solved analytically, e.g., for all transversely isotropic materials with any spatial orientation [35,36], and also for some classes of orthotropic materials [33].

Noteworthy, as follows from the procedure presented, all elements of the matrix $\mathbf{K}_{\text{corner}}(\lambda)$ are complex analytic (holomorphic) functions of λ , thus, also the determinant of this matrix is a complex analytic function of λ . Nevertheless, an analytic solution of (94) is not possible in general case, except for very specific simple cases. Even in the case of a single isotropic material, in plane strain, with free boundary faces, (94) is a transcendental equation requiring a numerical solution [3]. For this reason, we use a numerical method called Muller method [37] to solve it. This is a standard iterative procedure suitable for searching for complex roots of complex analytic functions.

Argument principle. To find all the roots of the complex-valued analytic function $\det \mathbf{K}_{\text{corner}}(\lambda)$ of λ inside a considered region of the complex plane, the Argument Principle [38] is also included in the code. The procedure indicates the number of roots (real and complex) in a region bounded by a closed contour C . This method counts the number of times the complex value of the analytic function $\det \mathbf{K}_{\text{corner}}(\lambda)$ rotates around the origin of the co-ordinate system, i.e. what is the multiple of 360° by which the argument of this function increases or decreases along the contour C :

$$J = \frac{1}{2\pi} [\arg(\det \mathbf{K}_{\text{corner}}(\lambda))]. \quad (95)$$

6. Stresses and displacements

Once that the *characteristic exponents* λ of a corner have been found, we can calculate the characteristic stress and displacement fields. First, we have to substitute the obtained λ value into the eigenequation (74) or (87) considering a fixed value of the radial coordinate r , e.g. $r = 1$. The solution for $\mathbf{w}_{\text{corner}_U}$, for this fixed value of $r = 1$, is a (right) null vector of the matrix $\mathbf{K}_{\text{corner}}(\lambda)$. As the obtained value for λ is substituted in $\mathbf{K}_{\text{corner}}(\lambda)$ we get a numerically defined matrix. To compute the null eigenvector of the numerically defined matrix $\mathbf{K}_{\text{corner}}(\lambda)$ we use the Singular Value Decomposition (SVD) giving the right singular vector of $\mathbf{K}_{\text{corner}}(\lambda)$ associated to the minimum singular value $\sigma_{\min} \approx 0$, which corresponds to $\mathbf{w}_{\text{corner}_U}$ for $r = 1$. The reason for using SVD is that sometimes we have found stability problems when computing the null eigenvector of $\mathbf{K}_{\text{corner}}(\lambda)$, whereas SVD has shown to be a very robust procedure for this purpose.

Next step is to complete $\mathbf{w}_{\text{corner}_U}$ with zero values of $\mathbf{w}_{\text{corner}_P}$ to get $\mathbf{w}_{\text{corner}_{PU}}$. Care must be taken with the size of the subvectors to be added, since as said before, for closed corners all subvectors \mathbf{w}_U are 6×1 vectors and so are the corresponding subvectors \mathbf{w}_P , but for open corners, the first and last subvectors \mathbf{w}_U are 3×1 vectors and the rest 6×1 vectors, the corresponding subvectors \mathbf{w}_P have the same size.

Introducing $\mathbf{w}_{\text{corner}_{PU}}$ in expression (71) or (84), we obtain $\mathbf{w}_{\text{corner}_{ext}}$. This vector contains the displacement and stress function for both faces of each wedge, $\mathbf{w}_w(r, \vartheta_{w-1})$ and $\mathbf{w}_w(r, \vartheta_w)$. The $\mathbf{w}_1(r, \vartheta_0)$ vector for the first face of the first wedge, corresponds directly to the $\mathbf{w}_1(r, \theta_0)$ vector of the first face of the first material of the first wedge. Using now the transfer matrix in (32), we get $\mathbf{w}_1(r, \theta_1)$ of the second face of the first material of the first wedge. As within a wedge we only have perfectly bonded interfaces, we know that the $\mathbf{w}_2(r, \theta_1)$ vector has the same values as $\mathbf{w}_1(r, \theta_1)$. Continuing with this process we can compute $\mathbf{w}_m(r, \theta_{m-1})$ for the first face of each material in the corner.

Now, starting with each $\mathbf{w}_m(r, \theta_{m-1})$ and using an analogous expression to (32), it is easy to get $\mathbf{w}_m(r, \theta)$ for each θ within each material,

$$\mathbf{w}_m(r, \theta) = \mathbf{E}_m(\lambda, \theta, \theta_{m-1}) \mathbf{w}_m(r, \theta_{m-1}) \quad \text{for } \theta_{m-1} \leq \theta \leq \theta_m. \quad (96)$$

Following the steps proposed by Ting [27, Section 7.3] the displacement vectors and stress tensor in cylindrical coordinates are:

$$u_r = -s_r^T(\theta) \mathbf{u}(r, \theta), \quad u_\theta = \mathbf{n}^T(\theta) \mathbf{u}(r, \theta), \quad u_3 = s_3^T(\theta) \mathbf{u}(r, \theta), \quad (97)$$

and

$$\begin{aligned} \sigma_{rr} &= \frac{s_r^T(\theta) \varphi_{,\theta}(r, \theta)}{r}, & \sigma_{\theta\theta} &= \mathbf{n}^T(\theta) \varphi_{,r}(r, \theta), \\ \sigma_{r\theta} &= \frac{-\mathbf{n}^T(\theta) \varphi_{,\theta}(r, \theta)}{r} = -s_r^T(\theta) \varphi_{,r}(r, \theta), \\ \sigma_{r3} &= \frac{-s_3^T(\theta) \varphi_{,\theta}(r, \theta)}{r}, & \sigma_{\theta 3} &= s_3^T(\theta) \varphi_{,r}(r, \theta), \end{aligned} \quad (98)$$

where the comma in the subscript stands for differentiation. We can get $\varphi_{,r}$ and $\varphi_{,\theta}$ from (30). On the one hand, as \mathbf{E} , \mathbf{X} , \mathbf{Z} and \mathbf{t} do not depend on r we have

$$\frac{\partial}{\partial r} \mathbf{w}(r, \theta) = \lambda r^{\lambda-1} \mathbf{XZ}^\lambda(\lambda, \theta, \theta_{m-1}) \mathbf{t} \quad (99)$$

for $\varphi_{,r}$. On the other hand, as \mathbf{E} depends on θ we have, for non-degenerate materials,

$$\frac{\partial}{\partial \theta} \mathbf{w}(r, \theta) = \frac{\partial}{\partial \theta} \mathbf{E}_m(\lambda, \theta, \theta_{m-1}) \mathbf{w}_m(r, \theta_{m-1}), \quad (100)$$

where

$$\frac{\partial}{\partial \theta} \mathbf{E}_m(\lambda, \theta, \theta_{m-1}) = \mathbf{X} \frac{\partial}{\partial \theta} \mathbf{Z}_m^\lambda(\lambda, \theta, \theta_{m-1}) \mathbf{X}^{-1}, \quad (101)$$

$$\frac{\partial}{\partial \theta} \mathbf{Z}_m^\lambda(\lambda, \theta, \theta_{m-1}) = \lambda \mathbf{Z}_m^{\lambda-1}(\lambda, \theta, \theta_{m-1}) \frac{\partial}{\partial \theta} \mathbf{Z}_m(\lambda, \theta, \theta_{m-1}) \quad (102)$$

$$\frac{\partial}{\partial \theta} \mathbf{Z}_m(\lambda, \theta, \theta_{m-1}) = \begin{bmatrix} \langle \zeta'_\alpha(\theta, \theta_{m-1}) \rangle & 0 \\ 0 & \langle \bar{\zeta}'_\alpha(\theta, \theta_{m-1}) \rangle \end{bmatrix}, \quad (103)$$

$$\zeta'_\alpha(\theta, \theta_{m-1}) = \frac{\partial}{\partial \theta} \zeta_\alpha(\theta, \theta_{m-1}) = -\sin(\theta - \theta_{m-1}) + p_\alpha(\theta_{m-1}) \cos(\theta - \theta_{m-1}). \quad (104)$$

These expressions allow us to compute stresses and displacements as functions of θ for a given value of r . An example to illustrate this procedure can be found in Section 8.3.

7. MATLAB implementation

The semianalytic procedure described above has been implemented in Matlab [23] using Symbolic Math Toolbox. This code calculates the singularity exponents and plots displacement and stress singular fields associated to a corner problem. The code is organized in 6 modules:

1. Data input
2. Definition of single-material wedges
3. Boundary and interface condition matrices
4. Characteristic system assembly
5. Solution of the characteristic system
6. Displacement and stress singular fields

7.1. Data input

The first module reads the data entered by the user and performs the necessary calculations. This module gives the user two options, to enter all the values that define the problem through a text file or interactively.

7.2. Material definition

This module is subdivided into three different functions, each function is for a type of material currently considered in the code. The options are isotropic, transversely isotropic or orthotropic. The code can be easily generalized to any other class of anisotropic materials, covering both, mathematically non-degenerated and degenerated materials following [8,20]. From the elastic constants and the initial and final angles for a single-material wedge number m , θ_{m-1} and θ_m respectively, the corresponding function will apply the Stroh formalism and store the *transfer matrix* $\mathbf{E}_m(\lambda)$ (33) as the definition of the single-material wedge.

This module is based on the theory described in Sections 2 and 3. Special attention was paid to the manipulation of angles and complex numbers to ensure the continuity of analytic functions as discussed in Section 3. In Matlab the function used to obtain the argument of a complex number is 'angle()' that returns the phase angle in the interval $\langle -\pi, \pi \rangle$. For the correct execution of (38), the following definition of 'arg()' function is used

$$\arg(z) \stackrel{\text{def}}{=} \begin{cases} \text{angle}(z) + 2\pi & \text{if } \text{angle}(z) \leq 0, \\ \text{angle}(z) & \text{if } \text{angle}(z) > 0. \end{cases} \quad (105)$$

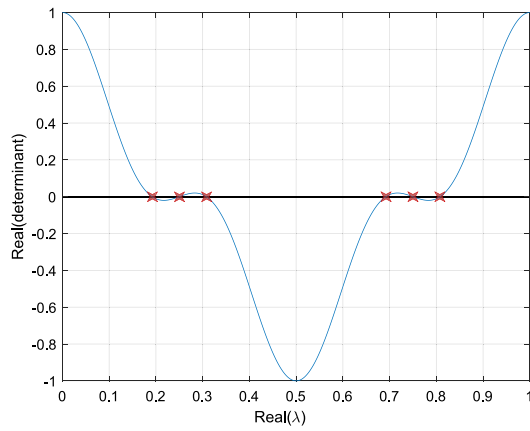


Fig. 4. Graphic representation of the real part of the determinant of the characteristic matrix of the multi-material corner. Example 1.12.

7.3. Boundary and interface condition matrices

The first step of this module is the creation of the right-handed reference frames (s_r, s_3, \mathbf{n}) attached to each face of the wedges that form the corner, see Fig. 2, and also ($\tilde{\mathbf{m}}, \tilde{\mathbf{l}}, \tilde{\mathbf{n}}$) for the cases of inclined planes shown in Fig. 3.

Once we have the reference frames defined for each angle at which a boundary or interface condition is prescribed, the boundary and interface condition matrices are generated depending on the type of boundary or interface condition, see Tables 1 and 2.

7.4. Characteristic system assembly

In this part, the \mathbf{K}_w matrix for each multi-material wedge (60) will be formed by the \mathbf{E}_m matrices (33) of the materials that form it. These \mathbf{K}_w matrices are combined with matrices \mathbf{D}_{BC} in (45) or \mathbf{D}_I in (51) generating the characteristic matrix $\mathbf{K}_{\text{corner}}(\lambda)$ for open corners (73) or for closed corners (86). Special attention is paid to the size of the rectangular and square matrices used in the assembly of the characteristic system.

7.5. Solution of the characteristic system

This module is based on Section 5.3. Once we have the characteristic matrix of the system $\mathbf{K}_{\text{corner}}(\lambda)$, (73) for open corners or (86) for closed corners, we initially define the interval of real values of λ where the roots of $\det \mathbf{K}_{\text{corner}}(\lambda)$ are searched for. This is the first part of the code where solution is numerical instead of analytical, since different values of λ will be substituted in the analytical expression of $\mathbf{K}_{\text{corner}}(\lambda)$ matrix to solve numerically the determinant. If the code detects that there may be a root between two of the λ values for which the determinant has been calculated, it will try to find a root in that interval using the Muller method [37]. After showing the roots automatically found, the software will show a graphic representation of $\text{Re}(\det \mathbf{K}_{\text{corner}}(\lambda))$ that could help the user to check the roots automatically found and indicate, in case that some root is missed, if new starting points for searching more roots are necessary. To illustrate this, the points where the curve intersects the abscissa axis in Fig. 4 are the points where the user should look for roots in case that the automatic procedure had not taken them into account.

The code also gives the option to run the submodule 'Argument Principle' to detect possible roots (real or complex) in a region of complex plane that have not been detected automatically.

7.6. Displacement and stress singular fields

At this point the code will perform the steps described in Section 6 to produce a graph like the one shown in Fig. 5. As can be seen from the formulas described in (98), for the calculation of stresses it is necessary to differentiate the stress function vector φ with respect to θ or r . To speed up the calculation, the analytical expression of each derivative has been used instead of leaving it to the software to derive it in each case. In the case of the derivative with respect to r , it is very simple, since according to the form of the expression of φ shown in (29), the differentiation with respect to r produces the same function φ multiplied by the root λ , considering $r = 1$, see (99). Slightly more complicated is the differentiation with respect to θ , for which we will have to differentiate with respect to θ the transfer matrix \mathbf{E}_m , which is the only part of the expression dependent on θ . The expression for the derivative of \mathbf{E}_m is computed directly from (101)–(104). Special care must be taken regarding the compatibility of dimensions of many vectors and matrices used in the procedure.

In the case a parameterization with respect to a corner parameter is requested, as in the example in Section 8.4, the code will repeat the modules 2 to 5 as many times as necessary.

8. Examples

To verify the correct implementation of the present procedure for corner singularity analysis in the developed code, many examples are solved and the results are compared with the numeric solution of the closed-form eigenequations available in the literature. In Table 3 we list, in the full precision considered, the characteristics of the used materials. For orthotropic materials, the fibers in the x_1x_3 -plane are oriented by angle ϕ with respect to the x_1 -axis. This angle is specified for each case of orthotropic material.

The studied problems are divided into open and closed corners and further subdivided into single-wedge and multi-wedge corners. The following acronyms are used: 'BC' Boundary Condition, 'IC' Interface Condition, 'B' perfectly Bonded, 'FL' FrictionLess, 'F' stress Free, 'C' Clamped, 'S' Symmetry, 'A' Antisymmetry, '(SY)' SYmmetric loading, '(SK)' SKew-symmetric loading, and '(A)' Antiplane shear. In the tables in this section, Example is abbreviated as 'Ex.' and material as 'Mat.' and the last column is CPU time in a workstation (DELL Precision 5550).

In most of the studied problems, the results found in the literature are usually for plane strain or plane stress only, whereas the presented formalism works in generalized plane strain. This means that this formalism in some cases finds solutions corresponding to the anti-plane shear that are not provided by some methods found in the literature. In those cases, in the corresponding table, the result obtained by the presented formalism is included beside a void cell corresponding to a result not covered by the eigenequation or closed-form expression for λ found in the literature

8.1. Solutions for open corners

8.1.1. Solutions for open corners with only one single-material or multi-material wedge

The expression for $\mathbf{K}_{\text{corner}}(\lambda)$ for this special case was deduced in Section 5.2.1.

Single-material wedge. If the wedge is made of only one material, then $\mathbf{K}_1(\lambda) = \mathbf{E}_1(\lambda)$ in (75). For isotropic materials, with stress free-stress free boundary conditions, results for λ are compared with those by Vasilopoulos [3] with perfect match. For isotropic materials with different homogeneous boundary conditions, we compare with the results obtained by the closed-form expressions collected by Sinclair [39]. In Table 4 we show some of these results.

The frictionless boundary condition corresponds to the symmetric boundary condition in the code, since it only restricts movement in the direction normal to the wedge face.

Table 3

Engineering constants for the materials used in the studied examples. Shear and elastic moduli in GPa.

Material	E_1	E_2	E_3	G_{12}	G_{13}	G_{23}	ν_{12}	ν_{13}	ν_{23}	ϕ
A	68.67						0.33			
B	3						0.35			
C	137.9	14.48	1	5.86	1	1	0.21	0	0	0
D	137.9	14.4795	14.4795	5.86	5.86	5.86	0.21	0.21	0.21	ϕ
E	137.9	14.48	14.48	4.98	4.98	4.98	0.21	0.21	0.21	ϕ
F	5.85						0.25			
G	141.3	9.58	9.58	5	5	3.5	0.3	0.3	0.32	ϕ

Table 4

Comparison with the results found in the literature for open single-material isotropic corners with different boundary conditions, Section 8.1.1.

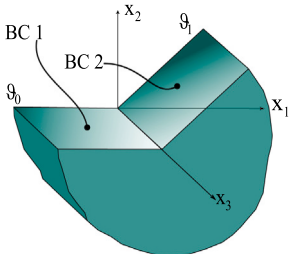
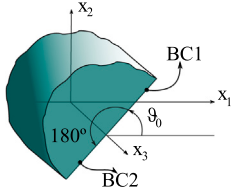
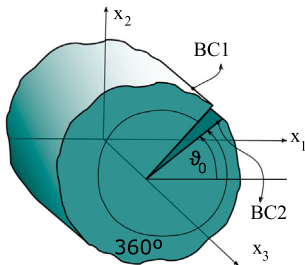
Corner configuration	Ex.	BC1	BC2	Mat	Results in literature [39]	Present results	Time (s)
	1.1	F/0°	F/270°	A	0.5444837368 (SY) 0.6666666667 (A) 0.9085291898 (SK)	0.5444837368 0.6666666667 0.9085291898	2.5
	1.2	F/0°	C/270°		0.3333333333 (A) 0.8607568402	0.3333333333 0.8607568402	3.1
	1.3	C/0°	C/270°		0.5904563986 (SK) 0.6666666667 (A) 0.7673218225 (SY)	0.5904563986 0.6666666667 0.7673218225	2.9
	1.4	FL/0°	FL/270°		0.3333333333 (SY) (SK) 0.6666666667 (A)	0.3333333333 (SY) (SK) 0.6666666667 (A)	3.1
	1.5	FL/0°	F/270°		0.3333333333 0.6666666667	0.3333333333 0.6666666667	2.9
	1.6	FL/0°	C/270°		0.3333333333 0.6666666667	0.3333333333 0.6666666667	3.0

Table 5

Comparison with the results found in the literature for open corner with only one orthotropic single-material wedge with different boundary conditions, Section 8.1.1.

Corner configuration	Ex.	BC1	BC2	Mat	Results in literature [32]	Present results	Time (s)
	1.7	F/ 20°	C/ 200°	C	$0.5 \pm 0.0994113836i$	$0.5 \pm 0.0994113836i$	2.2
	1.8	F or C/20°	S or A/200°		0.5	0.5	1.9
	1.9	S/20°	A/200°		0.3839541207 0.6160458793	0.3839541207 0.6160458793	2.7
	1.10	F/-340°	C/20°	C	$0.25 \pm 0.0497056918i$ $0.75 \pm 0.0497056918i$	$0.25 \pm 0.0497056918i$ $0.75 \pm 0.0497056918i$	2.2
	1.11	F or C/-340°	S or A/20°		0.25 0.5 0.75	0.25 0.5 0.75	3.1
	1.12	S/-340°	A/20°		0.1919770604 0.3080229396 0.6919770603	0.1919770604 0.3080229396 0.6919770603	3.9
					0.8080229396	0.8080229396	

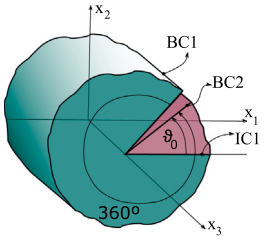
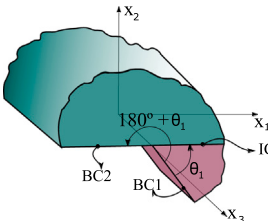
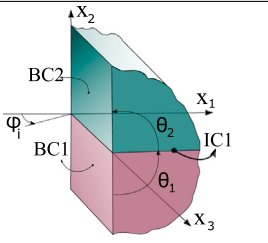
For orthotropic materials with different homogeneous boundary conditions, the results are compared with those obtained from the closed-form expression presented by Mantić et al. [32], see Table 5.

In Fig. 4, it is easy to identify the 6 real roots of the determinant solution of Example 1.12.

Multi-material and single-wedge corner. If there is only one wedge in the corner, but the wedge is made of several materials, the matrix of the corner eigenproblem to be solved is also (75).

Several examples of this kind of problem are solved comparing the results obtained by our code with those from different closed-form expressions. Some of these results are shown in Table 6 for two

Table 6
Comparison with the results found in the literature for a multi-material single-wedge corners, Section 8.1.1.

Corner configuration	Ex. [Ref.]	BC1 BC2	IC1	Mat.1 ϕ	Mat.2 ϕ	Results in literature [10,40,41]	Present results	Time (s)
	1.13 [40]	F/60° F/420°	B/360°			0.5116702380 0.7012296137 0.9274531170	0.5116702380 0.5941068002 0.7012296137 0.9274531170	15.1
	1.14 [40]	C/60° C/420°	B/360°	A	B	0.3362568013 ± 0.0362031284i 0.8253772310	0.3362568013 ± 0.0362031284i 0.8253772310 0.9055893170	14.2
	1.15 [40]	F/60° C/420°	B/360°			0.0812530200 0.1113639230 0.5407904749 0.7326576853	0.0812530200 0.0854358803 0.1113639230 0.5407904749 0.6110310672 0.7326576853	15.6
	1.16 [10]	F/0° C/240°	B/180°			0.0953560579 0.1634925888	0.0953560579 0.1117298041 0.1634925888	12.9
	1.17 [10]	A/0° C/240°	B/180°	A	B	0.1479273432 0.5224535404 0.5235945039	0.1479273432 0.5224535404 0.5235945039	11.1
	1.18 [10]	A/0° A/240°	B/180°			0.5	0.0888849178 0.5 0.5224535403	11.8
	1.19 [41]	F/240° F/450°	B/360°	D 15°	D 105°	0.9697	0.9697255043	81.1
	1.20 [41]	F/240° F/450°	B/360°	D 45°	D 105°	0.9869	0.9869011826	86.1
	1.21 [41]	F/240° F/450°	B/360°	D 75°	D 105°	0.9994	0.9993569674	74.8

materials. The results for Ex. 1.13, 1.14 and 1.15 have been compared with the results obtained from an analytic expression in Eq. (7) in [40].¹

The results for Ex. 1.16, 1.17 and 1.18, are compared with the results obtained from closed-form expression of eigenequation in [10]. The results for Ex. 1.19, 1.20 and 1.21 are compared with the values shown in Table 1 in [41]. In this case, Poonsawat et al. [41] show values of $\delta = 1 - \lambda$.

A special case of a crack meeting a perfectly bonded interface with an arbitrary angle was studied by various authors. In Table 7 we compare the results by the code with the results obtained from the closed-form equation presented by Bogy [42] for isotropic materials and with the results presented by Chen [43] for anisotropic materials.

8.1.2. Solutions for multi-material and multi-wedge open corners

In this case, we have more than one single-material or multi-material wedge. All the problems studied in Table 6 can be considered also in this section, since each material of a multi-material wedge can

¹ We would like to comment, as an aid to other researchers, that a typographical error was found in [40] that leads to wrong results when using Eq. (7) presented in that article. The original expression

$$\Delta_1 = (1 + u_2)^2 H(\varphi, 1, \lambda) + \Gamma^2 (1 + u_1^2) H(\varphi - 2\pi, 1, \lambda)...$$

should be replaced by the correct one

$$\Delta_1 = (1 + u_2)^2 H(\varphi, 1, \lambda) + \Gamma^2 (1 + u_1)^2 H(\varphi - 2\pi, 1, \lambda)...$$

be handled as a wedge. This is a way to verify the present matrix formalism and its computational implementation, since to solve problems of the last section, the determinants to be solved are for 6×6 matrices while the determinants to be solved for those problems considering each material as a wedge, are for $6M \times 6M$ matrices. Examples from 1.13 to 1.21 are solved again as multi-wedge corners instead of as single wedge corners. In both ways, we get the same results, helping us to verify the correct performance of the code.

In Table 8 examples with friction-less sliding contact are shown. The results for Ex. 2.1 and 2.2 obtained by the code are compared with [44], and for Ex. 2.3 and 2.4, respectively, with the data read from Figs. 3 and 4 in [45].² Some differences can be observed in the results for Ex. 2.3 and 2.4. However if we compare the results by our code and by solving the corrected equation in [45] (see the footnote 2) a perfect agreement is achieved.

² There is a misprint in [45] in Eq. (35), where it says

$$\frac{\sin \varphi}{\cos \varphi} = \frac{f \cos \varphi [w_{11}(\delta) + \hat{w}_{11}(\delta)] - [w_{12}(\delta) + \hat{w}_{12}(\delta)] + f \sin \varphi [w_{13}(\delta) + \hat{w}_{13}(\delta)]}{f \cos \varphi [w_{31}(\delta) + \hat{w}_{31}(\delta)] - [w_{32}(\delta) + \hat{w}_{32}(\delta)] + f \sin \varphi [w_{33}(\delta) + \hat{w}_{33}(\delta)]}$$

it should say

$$\frac{\sin \varphi}{\cos \varphi} = \frac{f \cos \varphi [w_{31}(\delta) + \hat{w}_{31}(\delta)] - [w_{32}(\delta) + \hat{w}_{32}(\delta)] + f \sin \varphi [w_{33}(\delta) + \hat{w}_{33}(\delta)]}{f \cos \varphi [w_{11}(\delta) + \hat{w}_{11}(\delta)] - [w_{12}(\delta) + \hat{w}_{12}(\delta)] + f \sin \varphi [w_{13}(\delta) + \hat{w}_{13}(\delta)]}$$

Table 7
Comparison with the results found in the literature for the case of a crack meeting a perfectly bonded interface, Section 8.1.1.

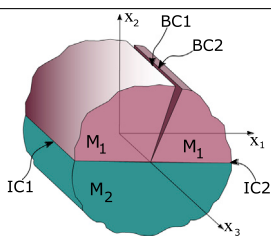
Corner configuration	Ex. [Ref.]	BC1 BC2	IC1 IC2	Mat.1 ϕ	Mat.2 ϕ	Results in literature [42,43]	Present results	Time (s)
	1.22 [42]	F/0° F/360°	B/135° B/315°	A 30°	B 150°	0.1355742073 0.3411304471	0.1355742073 0.1489730722 0.3411304471	46.3
	1.23 [43]	F/0° F/360°	B/90° B/270°	D 30°	D 150°	0.33749 0.505162 0.652054	0.3374847738 0.5051608017 0.6520577716	223.4

Table 8
Comparison with the results found in the literature for the case of a frictionless interface, Section 8.1.2.

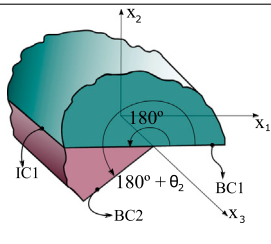
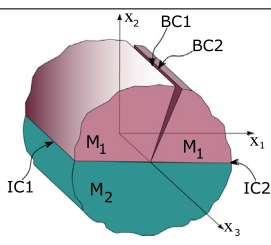
Corner configuration	Ex. [Ref.]	BC1 BC2	IC1 IC2	Mat.1 ϕ	Mat.2 ϕ	Results in literature [44,45]	Present results	Time (s)
	2.1 [44]	F/-180° F/180°	FL/0°	A 45°	B 0°	0.5	0.5	5.7
	2.2 [44]	F/-180° F/60°	FL/0°	B 45°	A 0°	0.6294574341	0.6294574341	8.6
	2.3 [45]	F/-180° F/90°	FL/0°	F 45°	E 90°	≈ 0.563	0.6753375590	12.3
	2.4 [45]	F/-180° F/120°	FL/0°	E 45°	E 0°	≈ 0.5687	0.5679983429	10.9

Table 9
Comparison with the results found in the literature for the case of a crack meeting a frictionless sliding interface, Section 8.1.2.

Corner configuration	Ex.	BC1 BC2	IC1 IC2	Mat.1 ϕ	Mat.2 ϕ	Results in literature [46]	Present results	Time (s)
	2.5	F/5° F/365°	FL/180° FL/360°			0.4997164050	0.4997164050	13.9
	2.6	F/45° F/405°	FL/0° FL/360°	A 45°	B 0°	0.3340154357	0.3340154357	12.3
	2.7	F/165° F/525°	FL/0° FL/360°			0.4922682295	0.4922682295	12.1

In examples shown in Table 9 there is a crack meeting an interface, similarly as in Table 7, but in these cases interfaces are frictionless. The results by the code for Ex. 2.5–2.7 are compared with the results shown by Gharpuray et al. [46].

8.2. Solutions for closed corners

8.2.1. Solutions for single-wedge closed corners

The cases studied here are either for corners where there are only perfectly bonded interface, or where all the interfaces are perfectly bonded except one of them that allows the frictionless sliding contact. Both cases are studied in Table 10. Ex. 3.1 shows a multi-material wedge where every interface is perfectly bonded, this example is compared with the numerical solution of the closed-form eigenequation introduced by Bogy [13]. Ex. 3.2 shows the same case but for an orthotropic material bonded to an isotropic material, this cases is studied by Barroso [47]. Ex. 3.3 shows the case of frictionless contact

between faces by Sung and Chung [48]. Ex. 3.4 shows the case of 3 orthotropic materials perfectly bonded studied by Chen [43]. In Ex. 3.5 and 3.6, one of the interfaces of the corner allows the frictionless sliding contact, this example is compared with the numerical solution of the closed-form eigenequation proposed by Comninou and Dundurs [49].³

³ There is a misprint in [49] Eq. (7). Where it says

$$P(\alpha) = (1 - \alpha)\beta,$$

it should say

$$P(\alpha) = (1 - \alpha)\beta.$$

Table 10
Comparison with the results found in the literature for the case of a single-wedge closed corner, Section 8.2.1.

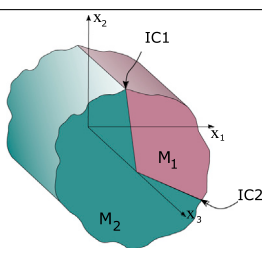
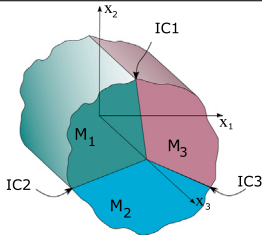
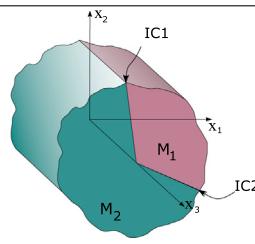
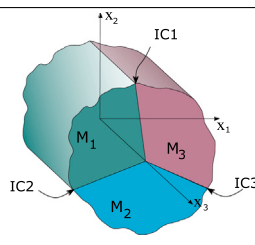
Corner configuration	Ex. [Ref.]	IC	Mat.1 ϕ	Mat.2 ϕ	Mat.3 ϕ	Results in literature [13,43,47–49]	Present results	Time (s)	
	3.1 [13]	B/0° B/135°	B	A		0.7016168738	0.7016168738 0.8153243783	20.5	
	3.2 [47]	B/0° B/90°	G 0°	B		0.763236 0.813696 0.889389 1.10698	0.7632362887 0.8136958777 0.8893886797 1.1069778843	28.5	
	3.3 [48]	B/0° FL/180°	D 0°	D 30°		0.5	0.5	7.1	
	3.4 [43]	B/90° B/180° B/270°	D 135°	D 45°	D 0°	0.917457	0.9174528878	150.2	
	3.5 [49]	B/0° B/180° FL/225°		A	B	B	0.7339773900	0.6563194237 0.7339773900	111.4
	3.6 [49]	B/0° B/180° FL/90°					0.6633562430	0.6633562430 0.8697736950	147.6

Table 11
Comparison with the results found in the literature for the case of multi-wedge closed corner, Section 8.2.2.

Corner configuration	Ex.	IC	Mat.1	Mat.2	Mat.3	Results in literature [50,51]	Present results	Time (s)
	4.1 [50]	FL/50° FL/310°	A	A		0.4583962335 0.6092455141	0.4583962335 0.6092455141 0.6923076923	9.1
	4.2 [50]	FL/75° FL/285°	A	A		0.1738393497 0.7321077798	0.1738393497 0.7321077798 0.8571428571	8.9
	4.3 [51]	FL/0° FL/120° FL/240°	A	A	A	0.55	0.5508138197	20.4

8.2.2. Solutions for multi-wedge closed corners

Corners with two or more wedges are studied in this section. In closed corners, as before for open corners, examples from 3.1 to 3.6 could be studied also as if the corner was made by several single-material wedges using the perfectly bonded interface condition instead of employing the multi-material transfer matrix. This exercise has been done to check the correct performance of the code. In Table 11, some examples of closed corners with more than one frictionless sliding interface condition are studied. In Ex. 4.1 and 4.2 the results obtained by the presented code are compared with those obtained from the closed-form eigenequation by Arias et al. [50] for this specific case. Ex. 4.3 makes a comparison between the obtained result and the result that Picu and Gupta [51] show in a plot. The examples in Table 11 are only dependent on the geometry, since the same result will be obtained for any isotropic material, as long as the corner is made only by one material.

8.3. Stresses and displacements

To show the capabilities of the developed code regarding the evaluation and graphical representation of the singular stress and displacement fields, we present their evolution around the corner for a special case of a corner under mode I of fracture, see Fig. 5. To simulate this behavior, we have studied an infinite semiplane of an orthotropic material G with $\phi = 0$ and with boundary conditions *only* u_1 allowed at $\vartheta_0 = 0$ and *only* u_3 restricted at $\vartheta_1 = \pi$. We will compare our values with those obtained from the expressions deduced in [52], see also [53].

8.4. Parametrization

The present code also offers the possibility of displaying the evolution of λ with respect to the variation of some corner parameters that may be of interest. Such evolution is shown in Fig. 6 for the variation of the singularity exponent, λ , as the angle γ , the angle that define the

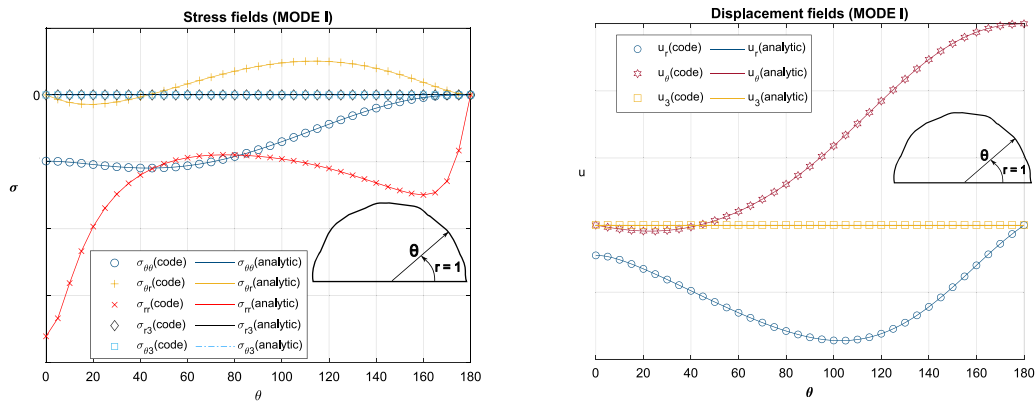


Fig. 5. Singular stress and displacement fields for orthotropic material G under fracture mode I. Results obtained from analytic expressions are represented by continuous lines, results obtained by the present code are represented by marks.

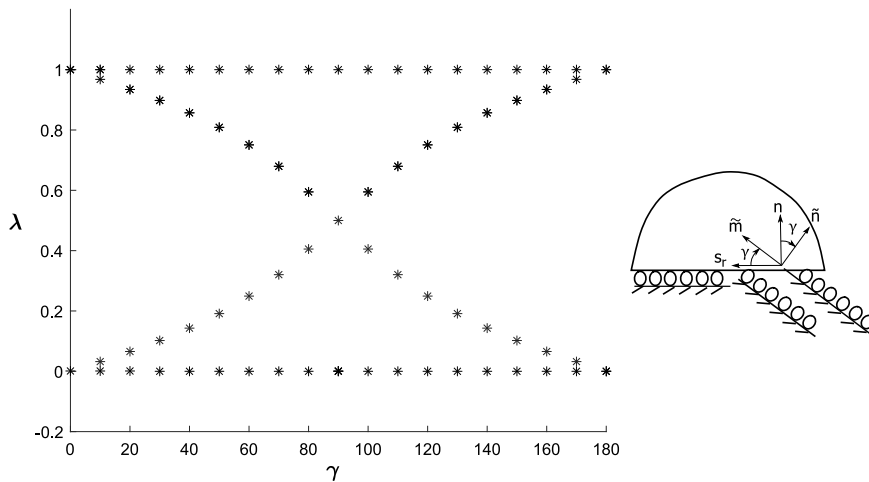


Fig. 6. Evolution of λ as γ increases.

vector \tilde{n} in the boundary condition *only $u_{\tilde{n}}$ restricted* (See Fig. 3), varies. In this example we have a single-material wedge of the orthotropic material D with $\phi = 0$, that goes from $\vartheta_0 = 0$, with boundary condition *only $u_{\tilde{n}}$ restricted*, to $\vartheta_1 = \pi$ with *symmetry* boundary condition, see Table 1.

9. Conclusions and future developments

This article revises and complements the matrix formalism and the computational procedure introduced in a very concise way in [8], in order to be easily understood by the readers. However, the most relevant contribution of the present article is that it presents the first general implementation of the proposed procedure, extensively and successfully tested by many numerical examples. This implementation allows us to verify the correct performance of the proposed matrix formalism too. The code has been validated through multiple tests comparing the obtained results with the results shown by other authors. This code has several advantages:

- Versatility, since it can solve a multitude of problems with essentially any useful boundary and interface conditions and any linear elastic material properties.
- Accuracy and reliability. It can be seen that all the numerical results computed by the code developed in the present work are essentially identical, at least up to 10 digits shown, to the results obtained by the numerical solution of closed-form eigenequations found in the literature. This excellent accuracy is a consequence of the semianalytic

character of the present procedure, where numerical solution is used to find roots of the sextic Lekhnitskii–Stroh characteristic polynomial of an anisotropic material if its solution in radicals is not possible, and to find roots of the transcendental eigenequation of the corner problem, where we are looking for roots of a complex-valued analytic (holomorphic) function of one complex variable. The rest of the calculations are fully analytical, providing the maximum accuracy to the present procedure. In fact, an arbitrary accuracy can be achieved using modern computer algebra software when working with numbers stored with an arbitrarily high precision.

- Ease of use and extension to study cases not considered in the current code version. Since the code is programmed by easily modifiable modules.
- An autocheck of this code can be performed in two different ways:
 - When rotating the corner, all θ will change, and with them also all relevant matrices. Despite this, the final results for λ and $w(r, \theta)$ have proven to be the same.
 - For a multi-material wedge, where there are one or more perfectly bonded interfaces, the formalism can be applied by using either the *perfectly bonded interface condition* or exploiting the *wedge transfer matrix*, and the result must be the same in both cases, even with substantially different sizes of the corner characteristic matrix.

The developed code is a general tool useful for researchers who need to know the singularity exponents and the singular stress fields to improve or check their numerical results by FEM, or to those researchers who need to verify their analytic formulas or eigenequations developed for specific corner singularity problems.

For this reason, in the near future, it is planned to share this tool as an online tool for the international research community. This code will be further developed by adding new functions like new boundary or interface conditions, especially friction contact boundary and interface conditions.

Declaration of competing interest

The authors declare that they have no known competing financial interests or personal relationships that could have appeared to influence the work reported in this paper.

Acknowledgments

The authors acknowledge that the code presented in this work is based on the code developed by Jara Allo, MSc in her Master's Thesis [54]. The research was conducted with the support of Spanish Ministry of Science, Innovation and Universities: PGC2018-099197-B-I00. Consejería de Transformación Económica, Industria, Conocimiento y Universidades, Junta de Andalucía: P18-FR-1928, US-1266016. European Regional Development Fund: PGC2018-099197-B-I00, P18-FR-1928, US-1266016.

Appendix A. Example of a boundary condition

Taking as example the case of *only* u_r restricted for a corner face at ϑ , where $\vartheta = \vartheta_0$ or ϑ_W , the Cartesian components of the vectors in (40) read

$$s_r(\vartheta) = \begin{pmatrix} -\cos(\vartheta) \\ -\sin(\vartheta) \\ 0 \end{pmatrix}, \quad s_3 = \begin{pmatrix} 0 \\ 0 \\ 1 \end{pmatrix}, \quad n(\vartheta) = \begin{pmatrix} -\sin(\vartheta) \\ \cos(\vartheta) \\ 0 \end{pmatrix}. \tag{106}$$

For this case (*only* u_r restricted)

$$D_u(\vartheta) = \begin{bmatrix} s_r^T(\vartheta) \\ \mathbf{0}_{1 \times 3} \\ \mathbf{0}_{1 \times 3} \end{bmatrix}, \quad \text{and} \quad D_\varphi(\vartheta) = \begin{bmatrix} \mathbf{0}_{1 \times 3} \\ n^T(\vartheta) \\ s_3^T \end{bmatrix}. \tag{107}$$

Now, by substituting (106) and (107) in expression (42):

$$\begin{bmatrix} -\cos(\vartheta) & -\sin(\vartheta) & 0 \\ 0 & 0 & 0 \\ 0 & 0 & 0 \end{bmatrix} \begin{bmatrix} u_1(r, \vartheta) \\ u_2(r, \vartheta) \\ u_3(r, \vartheta) \end{bmatrix} + \begin{bmatrix} 0 & 0 & 0 \\ -\sin(\vartheta) & \cos(\vartheta) & 0 \\ 0 & 0 & 1 \end{bmatrix} \begin{bmatrix} \varphi_1(r, \vartheta) \\ \varphi_2(r, \vartheta) \\ \varphi_3(r, \vartheta) \end{bmatrix} = 0, \tag{108}$$

we obtain

$$\begin{aligned} -\cos(\vartheta)u_1(r, \vartheta) - \sin(\vartheta)u_2(r, \vartheta) &= 0, \\ -\sin(\vartheta)\varphi_1(r, \vartheta) + \cos(\vartheta)\varphi_2(r, \vartheta) &= 0, \\ \varphi_3(r, \vartheta) &= 0. \end{aligned} \tag{109}$$

By writing the left hand side of these equations in polar coordinates we get

$$\begin{aligned} u_r(r, \vartheta) &= 0, \\ \varphi_\theta(r, \vartheta) = 0 &\Rightarrow \sigma_{\theta\theta}(r, \vartheta) = 0, \\ \varphi_3(r, \vartheta) = 0 &\Rightarrow \sigma_{\theta 3}(r, \vartheta) = 0. \end{aligned} \tag{110}$$

These results match with the expected boundary conditions for *only* u_r restricted conditions.

To see how expression (47) works, we can analyze it using the above example. First, we assemble the matrix $D_{BC}(\vartheta)$,

$$\begin{aligned} D_{BC}(\vartheta) &= \begin{bmatrix} \begin{pmatrix} s_r^T(\vartheta) \\ \mathbf{0}_{1 \times 3} \\ \mathbf{0}_{1 \times 3} \end{pmatrix} & \begin{pmatrix} \mathbf{0}_{1 \times 3} \\ n^T(\vartheta) \\ s_3^T \end{pmatrix} \\ \begin{pmatrix} \mathbf{0}_{1 \times 3} \\ n^T(\vartheta) \\ s_3^T \end{pmatrix} & \begin{pmatrix} s_r^T(\vartheta) \\ \mathbf{0}_{1 \times 3} \\ \mathbf{0}_{1 \times 3} \end{pmatrix} \end{bmatrix} \\ &= \begin{bmatrix} \begin{pmatrix} -\cos(\vartheta) & -\sin(\vartheta) & 0 \\ 0 & 0 & 0 \\ 0 & 0 & 0 \end{pmatrix} & \begin{pmatrix} 0 & 0 & 0 \\ -\sin(\vartheta) & \cos(\vartheta) & 0 \\ 0 & 0 & 1 \end{pmatrix} \\ \begin{pmatrix} 0 & 0 & 0 \\ -\sin(\vartheta) & \cos(\vartheta) & 0 \\ 0 & 0 & 1 \end{pmatrix} & \begin{pmatrix} -\cos(\vartheta) & -\sin(\vartheta) & 0 \\ 0 & 0 & 0 \\ 0 & 0 & 0 \end{pmatrix} \end{bmatrix}, \tag{111} \end{aligned}$$

then we substitute it in (47) leading to

$$\begin{aligned} &\begin{bmatrix} -\cos(\vartheta) & -\sin(\vartheta) & 0 & 0 & 0 & 0 \\ 0 & 0 & 0 & -\sin(\vartheta) & \cos(\vartheta) & 0 \\ 0 & 0 & 0 & 0 & 0 & 1 \\ 0 & 0 & 0 & -\cos(\vartheta) & -\sin(\vartheta) & 0 \\ -\sin(\vartheta) & \cos(\vartheta) & 0 & 0 & 0 & 0 \\ 0 & 0 & 1 & 0 & 0 & 0 \end{bmatrix} \begin{bmatrix} u_1(r, \vartheta) \\ u_2(r, \vartheta) \\ u_3(r, \vartheta) \\ \varphi_1(r, \vartheta) \\ \varphi_2(r, \vartheta) \\ \varphi_3(r, \vartheta) \end{bmatrix} \\ &= \begin{bmatrix} -\cos(\vartheta)u_1(r, \vartheta) - \sin(\vartheta)u_2(r, \vartheta) \\ -\sin(\vartheta)\varphi_1(r, \vartheta) + \cos(\vartheta)\varphi_2(r, \vartheta) \\ \varphi_3(r, \vartheta) \\ -\cos(\vartheta)\varphi_1(r, \vartheta) - \sin(\vartheta)\varphi_2(r, \vartheta) \\ -\sin(\vartheta)u_1(r, \vartheta) + \cos(\vartheta)u_2(r, \vartheta) \\ u_3(r, \vartheta) \end{bmatrix} \tag{112} \end{aligned}$$

and with (109)

$$\begin{aligned} &\begin{bmatrix} -\cos(\vartheta)u_1(r, \vartheta) - \sin(\vartheta)u_2(r, \vartheta) \\ -\sin(\vartheta)\varphi_1(r, \vartheta) + \cos(\vartheta)\varphi_2(r, \vartheta) \\ \varphi_3(r, \vartheta) \\ -\cos(\vartheta)\varphi_1(r, \vartheta) - \sin(\vartheta)\varphi_2(r, \vartheta) \\ -\sin(\vartheta)u_1(r, \vartheta) + \cos(\vartheta)u_2(r, \vartheta) \\ u_3(r, \vartheta) \end{bmatrix} = \begin{bmatrix} 0 \\ 0 \\ 0 \\ -\cos(\vartheta)\varphi_1(r, \vartheta) - \sin(\vartheta)\varphi_2(r, \vartheta) \\ -\sin(\vartheta)u_1(r, \vartheta) + \cos(\vartheta)u_2(r, \vartheta) \\ u_3(r, \vartheta) \end{bmatrix} \\ &= \begin{bmatrix} w_P(r, \vartheta) \\ w_U(r, \vartheta) \end{bmatrix}, \tag{113} \end{aligned}$$

we get the separation of the components of $w(r, \vartheta)$ into the prescribed ($u_r, \varphi_\theta, \varphi_3$) and unknown (φ_r, u_θ, u_3) components.

Appendix B. Example of an interface condition

The most difficult case of interface conditions dealt in this work is the case of frictionless sliding interface. Considering the same orthonormal basis as in (106), the matrices in Table 2 for this interface condition take the form

$$D_1(\vartheta) = \frac{1}{\sqrt{2}} \begin{bmatrix} \sin(\vartheta) & -\cos(\vartheta) & 0 & 0 & 0 & 0 \\ 0 & 0 & 0 & -\cos(\vartheta) & -\sin(\vartheta) & 0 \\ 0 & 0 & 0 & -1 & 0 & 0 \\ 0 & 0 & 0 & 0 & -1 & 0 \\ 0 & 0 & 0 & 0 & 0 & -1 \\ 0 & 0 & 0 & 0 & 0 & 1 \end{bmatrix}, \tag{114}$$

$$D_2(\vartheta) = \frac{1}{\sqrt{2}} \begin{bmatrix} -\sin(\vartheta) & \cos(\vartheta) & 0 & 0 & 0 & 0 \\ 0 & 0 & 0 & -\cos(\vartheta) & -\sin(\vartheta) & 0 \\ 0 & 0 & 0 & 1 & 0 & 0 \\ 0 & 0 & 0 & 0 & 1 & 0 \\ 0 & 0 & 0 & 0 & 0 & 1 \\ 0 & 0 & 0 & 0 & 0 & 1 \end{bmatrix}, \tag{115}$$

$$\tilde{\mathbf{D}}_1(\vartheta) = \frac{1}{\sqrt{2}} \begin{bmatrix} -\sin(\vartheta) & \cos(\vartheta) & 0 & 0 & 0 & 0 \\ 0 & 0 & 0 & -\sin(\vartheta) & \cos(\vartheta) & 0 \\ -\sqrt{2}\cos(\vartheta) & -\sqrt{2}\sin(\vartheta) & 0 & 0 & 0 & 0 \\ 0 & 0 & 0 & 0 & 0 & 0 \\ 0 & 0 & \sqrt{2} & 0 & 0 & 0 \\ 0 & 0 & 0 & 0 & 0 & 0 \end{bmatrix}, \quad (116)$$

$$\tilde{\mathbf{D}}_2(\vartheta) = \frac{1}{\sqrt{2}} \begin{bmatrix} -\sin(\vartheta) & \cos(\vartheta) & 0 & 0 & 0 & 0 \\ 0 & 0 & 0 & -\sin(\vartheta) & \cos(\vartheta) & 0 \\ -\sqrt{2}\cos(\vartheta) & -\sqrt{2}\sin(\vartheta) & 0 & 0 & 0 & 0 \\ 0 & 0 & 0 & 0 & 0 & 0 \\ 0 & 0 & 0 & 0 & 0 & 0 \\ 0 & 0 & \sqrt{2} & 0 & 0 & 0 \end{bmatrix}. \quad (117)$$

By substituting now (114) and (115) into (49) we obtain

$$\frac{1}{\sqrt{2}} \begin{bmatrix} \sin(\vartheta) & -\cos(\vartheta) & 0 & 0 & 0 & 0 \\ 0 & 0 & 0 & -\cos(\vartheta) & -\sin(\vartheta) & 0 \\ 0 & 0 & 0 & -1 & 0 & 0 \\ 0 & 0 & 0 & 0 & -1 & 0 \\ 0 & 0 & 0 & 0 & 0 & -1 \\ 0 & 0 & 0 & 0 & 0 & 1 \end{bmatrix} \begin{bmatrix} u_1^w(r, \vartheta) \\ u_2^w(r, \vartheta) \\ u_3^w(r, \vartheta) \\ \varphi_1^w(r, \vartheta) \\ \varphi_2^w(r, \vartheta) \\ \varphi_3^w(r, \vartheta) \end{bmatrix} + \frac{1}{\sqrt{2}} \begin{bmatrix} -\sin(\vartheta) & \cos(\vartheta) & 0 & 0 & 0 & 0 \\ 0 & 0 & 0 & -\cos(\vartheta) & -\sin(\vartheta) & 0 \\ 0 & 0 & 0 & 1 & 0 & 0 \\ 0 & 0 & 0 & 0 & 1 & 0 \\ 0 & 0 & 0 & 0 & 0 & 1 \\ 0 & 0 & 0 & 0 & 0 & 1 \end{bmatrix} \begin{bmatrix} u_1^{w+1}(r, \vartheta) \\ u_2^{w+1}(r, \vartheta) \\ u_3^{w+1}(r, \vartheta) \\ \varphi_1^{w+1}(r, \vartheta) \\ \varphi_2^{w+1}(r, \vartheta) \\ \varphi_3^{w+1}(r, \vartheta) \end{bmatrix} = \mathbf{0}. \quad (118)$$

where superindices w and $w + 1$ refer to two consecutive wedges, and $\vartheta = \vartheta_w$. By multiplying the vectors and matrices in (118) we get the interface conditions in explicit form

$$\begin{aligned} \frac{1}{\sqrt{2}}(\sin(\vartheta)u_1^w(r, \vartheta) - \cos(\vartheta)u_2^w(r, \vartheta) - \sin(\vartheta)u_1^{w+1}(r, \vartheta) \\ + \cos(\vartheta)u_2^{w+1}(r, \vartheta)) &= 0, \\ \frac{1}{\sqrt{2}}(-\cos(\vartheta)\varphi_1^w(r, \vartheta) - \sin(\vartheta)\varphi_2^w(r, \vartheta) - \cos(\vartheta)\varphi_1^{w+1}(r, \vartheta) \\ - \sin(\vartheta)\varphi_2^{w+1}(r, \vartheta)) &= 0, \\ \frac{1}{\sqrt{2}}(-\varphi_1^w(r, \vartheta) + \varphi_1^{w+1}(r, \vartheta)) &= 0, \\ \frac{1}{\sqrt{2}}(-\varphi_2^w(r, \vartheta) + \varphi_2^{w+1}(r, \vartheta)) &= 0, \\ \frac{1}{\sqrt{2}}(-\varphi_3^w(r, \vartheta) + \varphi_3^{w+1}(r, \vartheta)) &= 0, \\ \frac{1}{\sqrt{2}}(\varphi_3^w(r, \vartheta) + \varphi_3^{w+1}(r, \vartheta)) &= 0. \end{aligned} \quad (119)$$

By rewriting these conditions in polar coordinates it is easy to see what these equations imply

$$u_\theta^w(r, \vartheta) = u_\theta^{w+1}(r, \vartheta), \quad (120)$$

$$\varphi_\theta^w(r, \vartheta) = \varphi_\theta^{w+1}(r, \vartheta) \Rightarrow \sigma_{\theta\theta}^w(r, \vartheta) = \sigma_{\theta\theta}^{w+1}(r, \vartheta), \quad (121)$$

$$\varphi_r^w(r, \vartheta) = \varphi_r^{w+1}(r, \vartheta) = 0 \Rightarrow \sigma_{\theta r}^w(r, \vartheta) = \sigma_{\theta r}^{w+1}(r, \vartheta) = 0, \quad (122)$$

$$\varphi_3^w(r, \vartheta) = \varphi_3^{w+1}(r, \vartheta) = 0 \Rightarrow \sigma_{\theta 3}^w(r, \vartheta) = \sigma_{\theta 3}^{w+1}(r, \vartheta) = 0. \quad (123)$$

To see how expression (53) works, we can analyze it using the above example. By substituting (114)–(117) in (53) we obtain Eq. (124) given

in Box III, where the separation between the prescribed and unknown interface variables can be clearly observed.

Rewriting $\mathbf{w}_U(r, \vartheta)$ in polar coordinates, it is easy to see which components are our six unknown variables (besides a coefficient $\frac{1}{\sqrt{2}}$):

$$-\sin(\vartheta)u_1^w(r, \vartheta) + \cos(\vartheta)u_2^w(r, \vartheta) - \sin(\vartheta)u_1^{w+1}(r, \vartheta) \\ = u_\theta^w(r, \vartheta) + u_\theta^{w+1}(r, \vartheta) = 2u_\theta^w(r, \vartheta), \quad (125)$$

$$-\sin(\vartheta)\varphi_1^w(r, \vartheta) + \cos(\vartheta)\varphi_2^w(r, \vartheta) - \sin(\vartheta)\varphi_1^{w+1}(r, \vartheta) + \cos(\vartheta)\varphi_2^{w+1}(r, \vartheta) \\ = \varphi_\theta^w(r, \vartheta) + \varphi_\theta^{w+1}(r, \vartheta) = 2\varphi_\theta^w(r, \vartheta), \quad (126)$$

$$-\sqrt{2}\cos(\vartheta)u_1^w(r, \vartheta) - \sqrt{2}\sin(\vartheta)u_2^w(r, \vartheta) = -\sqrt{2}u_r^w(r, \vartheta), \quad (127)$$

besides $u_3^w(r, \vartheta)$, and similarly also $u_r^{w+1}(r, \vartheta)$ and $u_3^{w+1}(r, \vartheta)$.

Appendix C. Orthogonality of extended interface condition matrix

To check the orthogonality of the matrix $\mathbf{D}_{\text{corner_ext}}$ for a closed (periodic) corner we have to prove that this matrix fulfills (65),

$$\mathbf{D}_{\text{corner_ext}}(\vartheta)\mathbf{D}_{\text{corner_ext}}^T(\vartheta) = \begin{bmatrix} \mathbf{D}_2(\vartheta_0) & \mathbf{0}_{6 \times 6} & \mathbf{0}_{6 \times 6} & \cdots & \mathbf{0}_{6 \times 6} & \mathbf{0}_{6 \times 6} & \mathbf{D}_1(\vartheta_W) \\ \mathbf{D}_2(\vartheta_0) & \mathbf{0}_{6 \times 6} & \mathbf{0}_{6 \times 6} & \cdots & \mathbf{0}_{6 \times 6} & \mathbf{0}_{6 \times 6} & \tilde{\mathbf{D}}_1(\vartheta_W) \\ \mathbf{0}_{6 \times 6} & \mathbf{D}_1(\vartheta_1) & \mathbf{D}_2(\vartheta_1) & \cdots & \mathbf{0}_{6 \times 6} & \mathbf{0}_{6 \times 6} & \mathbf{0}_{6 \times 6} \\ \mathbf{0}_{6 \times 6} & \tilde{\mathbf{D}}_1(\vartheta_1) & \tilde{\mathbf{D}}_2(\vartheta_1) & \cdots & \mathbf{0}_{6 \times 6} & \mathbf{0}_{6 \times 6} & \mathbf{0}_{6 \times 6} \\ \vdots & \vdots & \vdots & \ddots & \vdots & \vdots & \vdots \\ \mathbf{0}_{6 \times 6} & \mathbf{0}_{6 \times 6} & \mathbf{0}_{6 \times 6} & \cdots & \mathbf{D}_1(\vartheta_{W-1}) & \mathbf{D}_2(\vartheta_{W-1}) & \mathbf{0}_{6 \times 6} \\ \mathbf{0}_{6 \times 6} & \mathbf{0}_{6 \times 6} & \mathbf{0}_{6 \times 6} & \cdots & \tilde{\mathbf{D}}_1(\vartheta_{W-1}) & \tilde{\mathbf{D}}_2(\vartheta_{W-1}) & \mathbf{0}_{6 \times 6} \end{bmatrix} \\ = \begin{bmatrix} \mathbf{D}_2^T(\vartheta_0) & \tilde{\mathbf{D}}_2^T(\vartheta_0) & \mathbf{0}_{6 \times 6} & \cdots & \mathbf{0}_{6 \times 6} & \mathbf{0}_{6 \times 6} & \mathbf{0}_{6 \times 6} \\ \mathbf{0}_{6 \times 6} & \mathbf{0}_{6 \times 6} & \mathbf{D}_1^T(\vartheta_1) & \tilde{\mathbf{D}}_1^T(\vartheta_1) & \cdots & \mathbf{0}_{6 \times 6} & \mathbf{0}_{6 \times 6} \\ \mathbf{0}_{6 \times 6} & \mathbf{0}_{6 \times 6} & \mathbf{D}_2^T(\vartheta_1) & \tilde{\mathbf{D}}_2^T(\vartheta_1) & \cdots & \mathbf{0}_{6 \times 6} & \mathbf{0}_{6 \times 6} \\ \vdots & \vdots & \vdots & \vdots & \ddots & \vdots & \vdots \\ \mathbf{0}_{6 \times 6} & \mathbf{0}_{6 \times 6} & \mathbf{0}_{6 \times 6} & \mathbf{0}_{6 \times 6} & \cdots & \mathbf{D}_1^T(\vartheta_{W-1}) & \tilde{\mathbf{D}}_1^T(\vartheta_{W-1}) \\ \mathbf{0}_{6 \times 6} & \mathbf{0}_{6 \times 6} & \mathbf{0}_{6 \times 6} & \mathbf{0}_{6 \times 6} & \cdots & \mathbf{D}_2^T(\vartheta_{W-1}) & \tilde{\mathbf{D}}_2^T(\vartheta_{W-1}) \\ \mathbf{D}_1^T(\vartheta_W) & \tilde{\mathbf{D}}_1^T(\vartheta_W) & \mathbf{0}_{6 \times 6} & \mathbf{0}_{6 \times 6} & \cdots & \mathbf{0}_{6 \times 6} & \mathbf{0}_{6 \times 6} \end{bmatrix} \\ = \begin{bmatrix} A & \mathbf{0}_{12 \times 12} & \cdots & \mathbf{0}_{12 \times 12} \\ \mathbf{0}_{12 \times 12} & B(\vartheta_1) & \cdots & \mathbf{0}_{12 \times 12} \\ \vdots & \vdots & \ddots & \vdots \\ \mathbf{0}_{12 \times 12} & \mathbf{0}_{12 \times 12} & \cdots & B(\vartheta_{W-1}) \end{bmatrix}, \quad (128)$$

where the 12×12 matrices A and $B(\vartheta_w)$ are given by

$$A = \begin{bmatrix} \mathbf{D}_2(\vartheta_0)\mathbf{D}_2^T(\vartheta_0) + \mathbf{D}_1(\vartheta_W)\mathbf{D}_1^T(\vartheta_W) & \mathbf{D}_2(\vartheta_0)\tilde{\mathbf{D}}_2^T(\vartheta_0) + \mathbf{D}_1(\vartheta_W)\tilde{\mathbf{D}}_1^T(\vartheta_W) \\ \tilde{\mathbf{D}}_2(\vartheta_0)\mathbf{D}_2^T(\vartheta_0) + \tilde{\mathbf{D}}_1(\vartheta_W)\mathbf{D}_1^T(\vartheta_W) & \tilde{\mathbf{D}}_2(\vartheta_0)\tilde{\mathbf{D}}_2^T(\vartheta_0) + \tilde{\mathbf{D}}_1(\vartheta_W)\tilde{\mathbf{D}}_1^T(\vartheta_W) \end{bmatrix} \\ = \begin{bmatrix} \mathbf{I}_{6 \times 6} & \mathbf{0}_{6 \times 6} \\ \mathbf{0}_{6 \times 6} & \mathbf{I}_{6 \times 6} \end{bmatrix}, \\ B(\vartheta_w) = \begin{bmatrix} \mathbf{D}_1(\vartheta_w)\mathbf{D}_1^T(\vartheta_w) + \mathbf{D}_2(\vartheta_w)\mathbf{D}_2^T(\vartheta_w) & \mathbf{D}_1(\vartheta_w)\tilde{\mathbf{D}}_1^T(\vartheta_w) + \mathbf{D}_2(\vartheta_w)\tilde{\mathbf{D}}_2^T(\vartheta_w) \\ \tilde{\mathbf{D}}_1(\vartheta_w)\mathbf{D}_1^T(\vartheta_w) + \tilde{\mathbf{D}}_2(\vartheta_w)\mathbf{D}_2^T(\vartheta_w) & \tilde{\mathbf{D}}_1(\vartheta_w)\tilde{\mathbf{D}}_1^T(\vartheta_w) + \tilde{\mathbf{D}}_2(\vartheta_w)\tilde{\mathbf{D}}_2^T(\vartheta_w) \end{bmatrix} \\ = \begin{bmatrix} \mathbf{I}_{6 \times 6} & \mathbf{0}_{6 \times 6} \\ \mathbf{0}_{6 \times 6} & \mathbf{I}_{6 \times 6} \end{bmatrix}, \quad (129)$$

where we have applied (50), using the fact that $\vartheta_0 + 360^\circ = \vartheta_W$, for a closed corner, in the matrix A calculation. This proves that the extended interface condition matrix fulfills the orthogonality relation (65).

$$\begin{aligned}
 & \frac{1}{\sqrt{2}} \begin{bmatrix} \sin(\vartheta) & -\cos(\vartheta) & 0 & 0 & 0 & 0 & -\sin(\vartheta) & \cos(\vartheta) & 0 & 0 & 0 & 0 \\ 0 & 0 & 0 & -\cos(\vartheta) & -\sin(\vartheta) & 0 & 0 & 0 & 0 & -\cos(\vartheta) & -\sin(\vartheta) & 0 \\ 0 & 0 & 0 & -1 & 0 & 0 & 0 & 0 & 0 & 1 & 0 & 0 \\ 0 & 0 & 0 & 0 & -1 & 0 & 0 & 0 & 0 & 0 & 1 & 0 \\ 0 & 0 & 0 & 0 & 0 & -1 & 0 & 0 & 0 & 0 & 0 & 1 \\ -\sin(\vartheta) & \cos(\vartheta) & 0 & 0 & 0 & 0 & -\sin(\vartheta) & \cos(\vartheta) & 0 & 0 & 0 & 0 \\ 0 & 0 & 0 & -\sin(\vartheta) & \cos(\vartheta) & 0 & 0 & 0 & 0 & -\sin(\vartheta) & \cos(\vartheta) & 0 \\ -\sqrt{2}\cos(\vartheta) & -\sqrt{2}\sin(\vartheta) & 0 & 0 & 0 & 0 & 0 & 0 & 0 & 0 & 0 & 0 \\ 0 & 0 & 0 & 0 & 0 & 0 & -\sqrt{2}\cos(\vartheta) & -\sqrt{2}\sin(\vartheta) & 0 & 0 & 0 & 0 \\ 0 & 0 & \sqrt{2} & 0 & 0 & 0 & 0 & 0 & 0 & 0 & 0 & 0 \\ 0 & 0 & 0 & 0 & 0 & 0 & 0 & 0 & \sqrt{2} & 0 & 0 & 0 \end{bmatrix} \\
 & \begin{bmatrix} u_1^w(r, \vartheta) \\ u_2^w(r, \vartheta) \\ u_3^w(r, \vartheta) \\ \varphi_1^w(r, \vartheta) \\ \varphi_2^w(r, \vartheta) \\ \varphi_3^w(r, \vartheta) \\ u_1^{w+1}(r, \vartheta) \\ u_2^{w+1}(r, \vartheta) \\ u_3^{w+1}(r, \vartheta) \\ \varphi_1^{w+1}(r, \vartheta) \\ \varphi_2^{w+1}(r, \vartheta) \\ \varphi_3^{w+1}(r, \vartheta) \end{bmatrix} = \frac{1}{\sqrt{2}} \begin{bmatrix} \sin(\vartheta)u_1^w(r, \vartheta) - \cos(\vartheta)u_2^w(r, \vartheta) - \sin(\vartheta)u_1^{w+1}(r, \vartheta) + \cos(\vartheta)u_2^{w+1}(r, \vartheta) \\ -\cos(\vartheta)\varphi_1^w(r, \vartheta) - \sin(\vartheta)\varphi_2^w(r, \vartheta) - \cos(\vartheta)\varphi_1^{w+1}(r, \vartheta) - \sin(\vartheta)\varphi_2^{w+1}(r, \vartheta) \\ -\varphi_1^w(r, \vartheta) + \varphi_1^{w+1}(r, \vartheta) \\ -\varphi_2^w(r, \vartheta) + \varphi_2^{w+1}(r, \vartheta) \\ -\varphi_3^w(r, \vartheta) + \varphi_3^{w+1}(r, \vartheta) \\ \varphi_3^w(r, \vartheta) + \varphi_3^{w+1}(r, \vartheta) \\ -\sin(\vartheta)u_1^w(r, \vartheta) + \cos(\vartheta)u_2^w(r, \vartheta) - \sin(\vartheta)u_1^{w+1}(r, \vartheta) + \cos(\vartheta)u_2^{w+1}(r, \vartheta) \\ -\sin(\vartheta)\varphi_1^w(r, \vartheta) + \cos(\vartheta)\varphi_2^w(r, \vartheta) - \sin(\vartheta)\varphi_1^{w+1}(r, \vartheta) + \cos(\vartheta)\varphi_2^{w+1}(r, \vartheta) \\ -\sqrt{2}\cos(\vartheta)u_1^w(r, \vartheta) - \sqrt{2}\sin(\vartheta)u_2^w(r, \vartheta) \\ -\sqrt{2}\cos(\vartheta)u_1^{w+1}(r, \vartheta) - \sqrt{2}\sin(\vartheta)u_2^{w+1}(r, \vartheta) \\ \sqrt{2}u_3^w(r, \vartheta) \\ \sqrt{2}u_3^{w+1}(r, \vartheta) \end{bmatrix} = \quad (124) \\
 & \frac{1}{\sqrt{2}} \begin{bmatrix} 0 \\ 0 \\ 0 \\ 0 \\ 0 \\ 0 \\ -\sin(\vartheta)u_1^w(r, \vartheta) + \cos(\vartheta)u_2^w(r, \vartheta) - \sin(\vartheta)u_1^{w+1}(r, \vartheta) + \cos(\vartheta)u_2^{w+1}(r, \vartheta) \\ -\sin(\vartheta)\varphi_1^w(r, \vartheta) + \cos(\vartheta)\varphi_2^w(r, \vartheta) - \sin(\vartheta)\varphi_1^{w+1}(r, \vartheta) + \cos(\vartheta)\varphi_2^{w+1}(r, \vartheta) \\ -\sqrt{2}\cos(\vartheta)u_1^w(r, \vartheta) - \sqrt{2}\sin(\vartheta)u_2^w(r, \vartheta) \\ -\sqrt{2}\cos(\vartheta)u_1^{w+1}(r, \vartheta) - \sqrt{2}\sin(\vartheta)u_2^{w+1}(r, \vartheta) \\ \sqrt{2}u_3^w(r, \vartheta) \\ \sqrt{2}u_3^{w+1}(r, \vartheta) \end{bmatrix} = \begin{bmatrix} \mathbf{w}_P(r, \vartheta) \\ \mathbf{w}_U(r, \vartheta) \end{bmatrix}
 \end{aligned}$$

Box III.

References

[1] K. Wieghardt, Über das Spalten und Zerreißen elastischer Körper (On splitting and cracking of elastic bodies) *Z. Angew. Math. Phys.* 55 (1–2) (1907) 60–103, Translation: Rossmanith H.P., *Fatigue Fract. Engng. Mater. Struct.* 12 (1995) 1371–1405.

[2] M.L. Williams, Stress singularities resulting from various boundary conditions in angular corners of plates in extension, *J. Appl. Mech.* 19 (1952) 526–528.

[3] D. Vasilopoulos, On the determination of higher order terms of singular elastic stress fields near corners, *Numer. Math.* 53 (1–2) (1988) 51–95.

[4] D. Leguillon, E. Sanchez-Palencia, *Computation of Singular Solutions in Elliptic Problems and Elasticity*, Masson, Paris, 1987.

[5] Z. Yosibash, *Singularities in Elliptic Boundary Value Problems and Elasticity and their Connection with Failure Initiation*, Springer, New York, 2012.

[6] J.P. Dempsey, G.B. Sinclair, On the stress singularities in the plane elasticity of the composite wedge, *J. Elasticity* 9 (4) (1979) 373–391.

[7] M. Costabel, M. Dauge, Y. Lafranche, Fast semi-analytic computation of elastic edge singularities, *Comput. Methods Appl. Mech. Engrg.* 190 (15) (2001) 2111–2134.

[8] V. Mantič, A. Barroso, F. París, Singular elastic solutions in anisotropic multi-material corners. Applications to composites, in: V. Mantič (Ed.), *Mathematical Methods and Models in Composites*, Imperial College Press, 2014, pp. 425–495.

[9] D.B. Bogy, K.C. Wang, Stress singularities at interface corners in bonded dissimilar isotropic elastic materials, *Int. J. Solids Struct.* 7 (8) (1971) 993–1005.

[10] J.P. Dempsey, G.B. Sinclair, On the singular behavior at the vertex of a bi-material wedge, *J. Elasticity* 11 (3) (1981) 317–327.

[11] C. Sator, W. Becker, Closed-form solutions for stress singularities at plane bi- and trimaterial junctions, *Arch. Appl. Mech.* 82 (5) (2012) 643–658.

[12] D.B. Bogy, The plane solution of anisotropic elastic wedges under normal and shear loading, *J. Appl. Mech.* 39 (4) (1972) 1103–1109.

[13] D.B. Bogy, Two edge-bonded elastic wedges of different materials and wedge angles under surface tractions, *J. Appl. Mech.* 38 (2) (1971) 377–386.

[14] T.C.T. Ting, S.C. Chou, Edge singularities in anisotropic composites, *Int. J. Solids Struct.* 17 (11) (1981) 1057–1068.

[15] K.-C. Wu, Near-tip field and the associated path-independent integrals for anisotropic composite wedges, *J. Mech.* 17 (1) (2001) 21–28.

[16] A.N. Stroh, Dislocations and cracks in anisotropic elasticity, *Philos. Mag. A J. Theor. Exp. Appl. Phys.* 3 (30) (1958) 625–646.

[17] A.N. Stroh, Steady state problems in anisotropic elasticity, *J. Math. Phys.* 41 (1–4) (1962) 77–103.

[18] C. Hwu, M. Omiya, K. Kishimoto, A key matrix N for the stress singularity of the anisotropic elastic composite wedges, *JSME Int. J. Ser. A Solid Mech. Mater. Eng.* 46 (01) (2003) 40–50.

[19] W.L. Yin, Anisotropic elasticity and multi-material singularities, *J. Elasticity* 71 (2003) 263–292.

[20] A. Barroso, V. Mantič, F. París, Singularity analysis of anisotropic multimaterial corners, *Int. J. Fract.* 119 (1) (2003) 1–23.

[21] S. Wolfram, *Mathematica, A System for Doing Mathematics by Computer*, Addison-Wesley, Redwood City, 1991.

[22] M. Steigemann, Power-law solutions of anisotropic multi-material elasticity problems, *J. Elasticity* 118 (2015) 63–87.

[23] C.B. Moler, *Numerical Computing with MATLAB*, Society for Industrial and Applied Mathematics, 2004.

- [24] T.C.T. Ting, Stress singularities at the tip of interfaces in polycrystals, in: H.P. Rossmannith (Ed.), *Damage and Failure of Interfaces*, Balkema Publishers, Rotterdam, 1997, pp. 75–82.
- [25] D.M. Barnett, H.O.K. Kirchner, A proof of the equivalence of the Stroh and Lekhnitskii sextic equations for plane anisotropic elastostatics, *Phil. Mag. A* 76 (1) (1997) 231–239.
- [26] S.G. Lekhnitskii, Some cases of the elastic equilibrium of a homogeneous cylinder with arbitrary anisotropy, *Appl. Math. Mech. (Prikl. Mat. Mekh.)* 2 (1938) 345–367, (in Russian).
- [27] T.C.T. Ting, *Anisotropic Elasticity: Theory and Applications*, Oxford University Press, New York, 1996.
- [28] V.A. Kondrat'ev, Boundary-value problems for elliptic equations in domains with conical or angular points, *Tr. Mosk. Mat. Obs.* 16 (1967) 209–292.
- [29] M. Costabel, M. Dauge, Construction of corner singularities for Agmon-Douglis-Nirenberg elliptic systems, *Math. Nachr.* 162 (1) (1993) 209–237.
- [30] C. Hwu, *Anisotropic Elasticity with Matlab*, Springer, Cham, 2021.
- [31] T.C.T. Ting, M.Z. Wang, Generalized Stroh formalism for anisotropic elasticity for general boundary conditions, *Acta Mech. Sinica* 8 (1992) 193–207.
- [32] V. Mantič, F. París, J. Cañas, Stress singularities in 2D orthotropic corners, *Int. J. Fract.* 83 (1997) 67–90.
- [33] G. Bonnet, Orthotropic elastic media having a closed form expression of the Green tensor, *Int. J. Solids Struct.* 46 (5) (2009) 1240–1250.
- [34] A.K. Head, The Galois unsolvability of the sextic equation of anisotropic elasticity, *J. Elasticity* 9 (1979) 9–20.
- [35] A. Barroso, V. Mantič, F. París, Computing stress singularities in transversely isotropic multimaterial corners by means of explicit expressions of the orthonormalized Stroh-eigenvectors, *Eng. Fract. Mech.* 76 (2) (2009) 250–268.
- [36] K. Tanuma, Surface-impedance tensor of transversely isotropic elastic materials, *Quart. J. Mech. Appl. Math.* 49 (1996) 29–48.
- [37] D.E. Muller, A method for solving algebraic equations using an automatic computer, *Math. Tables Aids Comput.* 10 (56) (1956) 208–215.
- [38] T. Johnson, W. Tucker, Enclosing all zeros of an analytic function — A rigorous approach, *J. Comput. Appl. Math.* 228 (1) (2009) 418–423.
- [39] G.B. Sinclair, Stress singularities in classical elasticity—I: Removal, interpretation and analysis, —II: Asymptotic identification, *Appl. Mech. Rev.* 57 (4) (2004) 251–297 and 385–439.
- [40] P.S. Theocaris, E.E. Gdoutos, Stress singularities in cracked composite full-planes, *Int. J. Fract.* 13 (6) (1977) 763–773.
- [41] P. Poonsawat, A.C. Wijeyewickrema, P. Karasudhi, Singular stress fields of angle-ply and monoclinic bimaterial wedges, *Int. J. Solids Struct.* 38 (2001) 91–113.
- [42] D.B. Bogy, On the plane elastostatic problem of a loaded crack terminating at a material interface, *J. Appl. Mech.* 38 (4) (1971) 911–918.
- [43] H.P. Chen, Stress singularities in anisotropic multimaterial wedges and junctions, *Int. J. Solids Struct.* 35 (11) (1998) 1057–1073.
- [44] E.E. Gdoutos, P.S. Theocaris, Stress concentrations at the apex of a plane indenter acting on an elastic half plane, *J. Appl. Mech.* 42 (3) (1975) 688–692.
- [45] H.P. Chen, Z. Guo, X. Zhou, Stress singularities of contact problems with a frictional interface in anisotropic bimaterials, *Fatigue Fract. Eng. Mater. Struct.* 35 (2012) 718–731.
- [46] V.M. Gharpuray, J. Dundurs, L.M. Keer, A crack terminating at a slipping interface between two materials, *J. Appl. Mech.* 58 (4) (1991) 960–963.
- [47] A. Barroso, Caracterización de estados singulares de tensión en esquinas multiamateriales. Aplicación a uniones adhesivas con materiales compuestos (Ph.D. thesis), Departamento de Mecánica de Medios Continuos, Teoría de Estructuras e Ingeniería del Terreno. Universidad de Sevilla, 2007.
- [48] J.C. Sung, W.G. Chung, Frictional interface crack in anisotropic bimaterial under combined shear and compression, *Int. J. Solids Struct.* 40 (24) (2003) 6839–6857.
- [49] M. Comninou, J. Dundurs, A closed crack tip terminating at an interface, *J. Appl. Mech.* 46 (1) (1979) 97–100.
- [50] R. Arias, R. Madariaga, M. Adda-Bedia, Singular elasto-static field near a fault king, *Pure Appl. Geophys.* 168 (12) (2011) 2167–2179.
- [51] C.R. Picu, V. Gupta, Stress singularities at triple junctions with freely sliding grains, *Int. J. Solids Struct.* 33 (11) (1996) 1535–1541.
- [52] G.C. Sih, P.C. Paris, G.R. Irwin, On cracks in rectilinearly anisotropic bodies, *Int. J. Fract. Mech.* 1 (1965) 189–203.
- [53] F.G. Yuan, *Lecture on Anisotropic Elasticity Application to Composite Fracture Mechanics*, Mechanics of Materials Branch, Hampton, 1998.
- [54] J. Allo Fernández de Tejada, Implementación de un código para el cálculo de singularidad de tensiones en esquinas multimateriales anisótropas (Trabajo Fin de Máster), Departamento de Mecánica de Medios Continuos, Teoría de Estructuras e Ingeniería del Terreno. Universidad de Sevilla, 2013.